LIVERPOOL

13 to 15 APRIL 2023

Invited Speaker Talk Summaries

Oral Presentation Abstracts

Poster Pitching Abstracts

BRS only Poster Abstracts

Overview of the BRS Annual Meeting 2023

The Bone Research Society (BRS), formerly the Bone and Tooth Society, was founded in 1950. The BRS is one of the largest national scientific societies in Europe dedicated to clinical and basic research into mineralised tissues and is the oldest such society in the world. Meetings are held annually, attracting a wide audience from throughout the UK and beyond. The presentations are traditionally balanced between clinical and laboratory studies. The participation of young scientists and clinicians is actively encouraged.

The 2023 Annual Meeting of the Bone Research Society (BRS) was held at the award-winning ACC in Liverpool from Thursday 13th to Saturday 15th April. The Meeting was held in association with the European Calcified Tissues Society (ECTS) Annual Congress, which then ran from Saturday 15th to Tuesday 18th April. The Societies joined forces to provide an exciting and unique opportunity to share cutting edge science and innovation in bone and mineral metabolism.

BRS held its usual pre meeting Workshops on Thursday 13th April to include the Rare Bone Disease workshop, Muscle and Bone workshop and the New Investigators workshop. We also added an additional Cancer and Bone workshop.

Delegates were invited to register for, and submit abstracts to, either or both meetings. There was a joint abstract submission process where authors could decide whether to submit their abstract to BRS alone or to ECTS and BRS.

There were two days with a full programme of invited speakers, debate, oral communications, posters presenting and two satellite symposia from our industry partners.

Topics covered were:

- Rare Bone Disease
- Muscle and Bone
- New approaches and techniques
- Emerging therapies
- Advances in cell biology
- Bone mechanoadaptation
- Cancer and bone
- Nutrition, the gut and bone

Local Organising Committee

Jim Gallagher (Liverpool, Chair)
Kate Ward (Southampton)
Kassim Javaid (Oxford)
Allie Gartland (Sheffield)
Alex Ireland (Manchester)
Juliette Hughes (Liverpool)
Scott Dillon (Cambridge)

Invited Speaker Talk Summaries

MB1.1

Evolutionary biomechanics: hard tissues and soft evidence?

Dr Karl Bates

Liverpool, UK

Summary

Changes in functional morphology have underpinned some of the most significant evolutionary transitions in the history of life. Colonization of the land by the earliest tetrapods, mammalian origins and diversification, the evolution of locomotion in dinosaurs and birds, and functional and ecological shifts in human ancestors represent extensively studied examples. The last two decades has seen widespread adoption of sophisticated mathematical-computational approaches to study functional morphology in extinct animals and the biomechanics of evolutionary transitions documented in the fossil record. These approaches realize a number of benefits relative to more traditional comparative approaches, particularly the ability to deliver absolute measures of functional performance in fossil animals (e.g. energy costs, maximal performance), thereby allowing quantitative tests of how anatomical innovations enabled major behavioural niche adaptions over geological time.

However, one challenging aspect in their use on extinct animals is that they require precise specification of numerical values for soft tissue parameters (e.g. muscle mass) that are rarely, or never, preserved in fossils. Research on extinct animals have subsequently employed a diverse range of approaches to estimate absolute values for soft tissue parameters like muscle mass and fibre length in fossils, but to-date very few of these studies have extensively validated their approaches on living animals. Here I present two case studies where research on living animals has been used to directly inform research into the movement capabilities of extinct animals through basic extrapolations from Newton's Second Law of Motion. In the first case study, reconstructions of mass properties have been used to infer changes in locomotion along the evolutionary lineage leading to modern birds. Here, living animals that phylogenetically bracket bird ancestors have been used to develop predictive relationships between skeletal and body segment volumes that allow the prediction of body mass and centre-of-mass in extinct dinosaurs based on 3D scans of their fossilised bone. I review how this method has recently been used to track the evolution of body shape and mass distribution through bird evolution to identify the origin of centre-of-mass positions more advantageous for flight and major reversions coincident with terrestriality.

My second case study examines the second element of Newton's Second Law – force – and specifically the accuracy of current methods used to constrain muscle force generating capacity in fossil animals and test macroevolutionary hypothesis based on biomechanical models. Here, we modelled the masticatory system in extant rodents to objectively test the ability of current muscle reconstruction methods to correctly identify quantitative and qualitative differences between macroevolutionary morphotypes (sciuromorphs, myomorphs and hystricomorphs). Predictions from models generated using reconstruction methods typically used in fossil studies varied widely from high levels of quantitative accuracy to a failure to correctly capture even relative differences between macroevolutionary

morphotypes. This novel experiment emphasizes that correctly reconstructing even qualitative differences between extinct taxa in a macroevolutionary radiation is challenging using current methods. Future studies should seek to expand primary datasets on muscle properties in extant taxa to better inform soft tissue reconstructions in macroevolutionary studies.

MB1.2

Human gait: the upright ape

Dr Kris D'Aout

Liverpool, UK

Summary

Humans are the only upright, bipedal primates, and this has led to a plethora of musculoskeletal adaptations due to changes in posture, gait and as a consequence, tissue loading. We will review some key characteristics of human gait biomechanics and how they are reflected anatomically. This will draw on fossil interpretation, modelling, and experimental work. For the latter we will include work on the use of extant primates such as bonobos and baboons to answer fundamental questions about the transition to bipedality in early hominins. We will also explore the study of human volunteers in the lab on a variety of substrates, and of diverse human populations in field settings.

The foot, our only mechanical interface with the environment during gait, plays a crucial role and the effect of footwear on its anatomy and function will be highlighted.

Our own and literature data highlight that the actual load on our musculoskeletal system (e.g., pressures, forces, joint moments) can be contradictory to intuition. For example, cushioned footwear has been shown in several studies to lead to higher, not lower, impact forces in athletics, daily activities, and disease, including knee and hip osteo-arthritis. In addition, the type of footwear we use (or not) has an effect on muscle force and balance and is therefore important both as a preventative measure throughout the life span and as an intervention in older age.

RBD1.3

Assessing rare bone diseases using Raman spectroscopy: a rare insight

Dr Jemma Kerns

Lancaster, UK

Summary

Raman spectroscopy is a laser-based technique that is both non-ionising and non-destructive, it is well established as a laboratory technique and is being explored for translational implementation, due to it's potential as a clinical tool. Lasers excite samples, providing energy, causing the molecular bonds to vibrate using a specific amount of energy e.g., a C-O stretch will use a different amount of energy to a C-H vibration. The outputting light will have shifted in energy and therefore wavelength, and may be plotted as a spectrum. Analysis of spectra from samples of interest permits the identification of any chemical differences between and within samples. The application of Raman spectroscopy to bone samples is particularly useful because many clinical techniques to measure bone can only collect reliable information from the mineral component of the bone. Osteogenesis imperfecta is a genetic condition where the protein component, collagen, is altered, causing the overall bone structure to become less able to withstand load, and fracture with minimal or no impact. In the first study presented here, an individual underwent a wedge osteotomy of her femur to straighten it, the wedge of bone that was removed was directly measured with Raman spectroscopy, and compared to a gender matched control. The patient also had spectral measurements of their tibia collected through the skin using spatially offset Raman spectroscopy (SORS). This data was compared to an age and gender matched control. Results from both sets of data show that the OI bone is more mineralised to the matched controls. Despite having using different instruments, bone and controls, the difference in mineralisation associated with OI is dominant.

In the second study, ear biopsies from people with alkaptonuria were measured with Raman spectroscopy. As part of the SOFIA trial, data was available about the amount of pigmentation present in each sample. The pigmentation in the samples caused a high degree of fluorescence, not completely unexpected, but this was utilised in analysis. Specifically, it showed a strong correlation between the degree of pigmentation and amount of fluorescence. Further analysis of the Raman spectral information with and without the fluorescence showed that it was possible to distinguish between the areas of non-pigmentation and high pigmentation, as well as the samples of semi- or mixed pigmentation.

Overall, Raman spectroscopy can measure chemical changes within and between samples, due to different medical conditions. This is important for both the development of diagnostic tools, and in furthering our understanding of these rare diseases, to hopefully aid in treatment development and monitoring, to improve quality of life.

RBD1.5

Fibrodyplasia ossificans progressiva

Professor Richard Keen

London, UK

Summary

Fibrodysplasia ossificans progressiva (FOP) is an ultra-rare autosomal genetic disorder, with an estimated global prevalence of approximately 0.61 to 1.43 per million individuals. The condition is caused by mutations within the Activin A receptor type 1 gene (ACVR1) which encodes a receptor in the bone morphogenetic protein (BMP) pathway. 97% of individuals with FOP have the same R206H mutation. This pathogenic variant increases BMP pathway signalling, which directs mesenchymal stem cells to chondrogenic and osteogenic fates, resulting in heterotopic ossification (HO) in muscles, tendons, ligaments, fascia, and aponeuroses.

The hallmark sign of FOP is a malformation of a newborn's big toe. This is apparent at birth and consists of a short big toe with a valgus deviation. In many cases, the link between the toe abnormalities and FOP is not made until the patient starts to experience characteristic disease flare-ups. These flares are painful, recurrent episodes of soft tissue swelling, and occur more frequently in the neck, trunk, and upper limbs before age 8 years and more frequently in the lower limbs thereafter. On average, 30% of these flare-ups can result in the formation of HO. This leads to a progressive and permanent restriction in movement and function. HO can also progress sub-clinically. Biopsies of the soft tissue swelling or attempted surgical removal of the HO will cause further disease flares and worsening of the patient's condition. In patients with suspected FOP, confirmation of the diagnosis can now be made with genetic analysis of the ACVR1 gene.

Although there is variability in the rate of disease progression, once ossification occurs, it is permanent. Most patients become immobilised and need to use a wheelchair by their 20s and require assistance to perform activities of daily living. Life-limiting complications of FOP include severe weight loss due to jaw ankylosis, thoracic insufficiency due to ankylosis of the costovertebral joints, ossification of the intercostal and paravertebral muscles, and progressive spinal deformity. Life expectancy is reduced.

At present there are no licensed or proven treatments that are effective in FOP. Management is mainly supportive. It is important to reduce risk of injury or trauma as these could precipitate disease flares. Iatrogenic procedures such as intramuscular injections or vaccines, dental blocks, biopsies and surgical procedures should also be avoided. Acute flare-ups are treated symptomatically with anti-inflammatory drugs. Short courses of high dose oral steroids are used for flares involving the neck, jaw and appendicular skeleton. These measures can help reduce pain and swelling, but there is no evidence that they reduce the development of HO.

Based on the molecular mechanism underlying FOP, there has been considerable progress in identification of possible therapeutic targets. A number of Phase 2 and Phase 3 trials are currently in progress. Outcome measures include the burden of whole body HO as assessed by CT imaging. Trials that demonstrate a reduction in HO, will subsequently need to show a positive impact on the longer term quality of life and physical functioning of individuals with FOP.

S1.1

Longitudinal growth, pubertal timing and bone health

Professor Tim Cole

London, UK

Summary

Age-related bone loss leads to lower bone density and an increased risk of osteoporosis and fragility fracture later in life. Poor bone health is a major societal issue: there were around 3.8 million new cases of osteoporosis in 2019, three-quarters of them women; the number is projected to rise appreciably over the next decade due to the ageing population, and the associated costs are substantial, representing around 2.4% of all healthcare spending in 2019, due to the high rates of morbidity and mortality. For all these reasons there is a need to better understand and treat osteoporosis.

Bone mass is accrued during childhood and peaks during the third or fourth decade of life. Subsequently bone absorption exceeds bone formation, leading to bone loss and an increasing risk of fragility fracture. Later bone mass is strongly influenced by peak bone mass, which in turn depends on the amount of bone accrued during the period of childhood growth.

For 30 years it has been known that later menarche in women is a risk factor for later osteoporosis and fragility fracture, and this is believed to extend to a more general association with the timing of puberty in both sexes. To explore this association in more depth requires assessing the timing of puberty in a cohort of individuals whose bone health in later life is also documented. Puberty timing can be estimated from the age of attainment of secondary sexual characteristics, notably menarche in girls, or Tanner staging. Growth in puberty provides an alternative, more objective and precise estimate of timing, albeit requiring longitudinal data, whereby growth models estimate individual height growth curves from which the age at peak height velocity can be obtained.

The talk focuses on ways of estimating age at peak velocity, notably parametric functions such as the growth curve model of Preece and Baines (1978), and the mixed effects hierarchical model SITAR (SuperImposition by Translation And Rotation) (Cole et al 2010). Both work well, though SITAR has some advantages. It is used to show that calcium supplementation in a rural African environment advances peak height velocity and reduces final height in boys. SITAR has also been used to quantify pubertal growth patterns in bone mineral content (BMC) relative to height (McCormack et al 2017).

As a life course example, the MRC National Study of Health and Development (NSHD or 1946 Cohort) provided data on child growth and later bone health, which was used to directly test the association between puberty timing and later BMC. The NSHD data needed boosting, using data from ALSPAC, due infrequent growth measurements in puberty. The results showed that trabecular vBMD as measured at age 60-64 was highly significantly inversely associated with the timing of puberty in both sexes 45-50 years earlier. This has important implications for the risk of fragility fracture in later life.

S1.2

Growth plate biology

Professor Katherine Staines

Brighton, UK

Summary

The growth plate is the developmental region located in the epiphysis and responsible for longitudinal bone growth. The epiphyseal growth plate chondrocytes have a transient phenotype - desirable to ensure long bone development (endochondral ossification) and growth. This is in contrast to the chondrocytes of the articular cartilage which have a stable phenotype to ensure the longevity of this tissue. Growth plate chondrocytes undergo a differentiation sequence of proliferation, maturation, and hypertrophy as is reflected by their changing morphology and matrix production. The final stage of cell hypertrophy enables mineralisation of the cartilage extracellular matrix, vascular invasion and subsequent replacement of the mineralised cartilage anlagen with bone. These processes are coupled, however, with sexual maturation the human growth plate undergoes progressive narrowing as bony bridges form and span its width. This ultimately leads to complete growth plate closure and cessation of human growth.

In this talk I will give an overview of the growth plate biology, with a particular focus on the fusion mechanisms. I will describe methods we have developed to understand these processes in a 3D context, and our programme of work aimed at understanding how these may predict musculoskeletal health in later life using murine models and human cohorts.

IL1

Equine Calcified Tissue Scrutineering. What have we learnt from the horse?

Professor Alan Boyd

London, UK

Summary

All equine mineralized tissues are remarkable and none more so than in the teeth, which must function before they anatomical roots. Bone is directly attached to mature dental enamel after its resorption by osteoclasts – the resulting bond of this coronal cementum with enamel is superior to anything yet achieved in with clinical restorative materials. Externally, this cement (bone) attaches the periodontal ligament to the alveolar bone: internally it fills erstwhile space and holds the tooth together: its osteocytes die and are unable to prevent mineralization: although dead, it is a functional dental tissue: it may be subject to irregular resorption prior to eruption -diagnosed as 'caries'. Horse enamel is extraordinary in demonstrating sub-daily growth rhythms. Big dentine tubules are pre-emptively filled with dense 'peritubular' dentine, which is relatively wear-resistant and generates microrelief at the occlusal surface.

Studies of compact cortical tissue in equine long bone shafts by quantitative circularly polarized light microscopy first revealed pronounced differences in preferred collagen orientation patterns and turnover between tension and compression cortices. Recent advances in computer driven linear polarized light microscopy provide more detailed analyses of 3D organization of bone matrix and its complexities during growth processes at ligament / tendon / aponeurosis loaded surfaces. We have even found Sharpey fibres within secondary osteons.

Several studies of groups of horses subjected to natural or imposed contrasting exercise level regimes have provided us with abundant information about physiological and pathological changes in bones which are more relevant to the human scene than that obtained from laboratory rodents. We have made detailed characterisations of the structure of differently loaded different types of skeletal tissue, practically none of which are correctly described in currently accepted teaching and demagogic research literature.

Grossly excessive levels of cyclical loading lead to real ruptures. Many fractures initiate in articular calcified cartilage (ACC): their propagation past subchondral bone (SCB) may be strongly favoured by an architecture of parallel plates: these large trabeculae contain an abundant blood vessel canal system, including secondary osteons, but also simple canals which incorporate pre-existing capillaries or are drilled by osteoclasts just to make enough space for one. Real damage initiates pathological resorption which expands the potential fracture path: this is a major feature of fatigue fractures and the initiation of lesions in overload osteoarthritis.

Acceptable, sensible increases in exercise cause densification of less-than-dense bone and reversal of resorption. When acute, the most abundant new bone deposition - both in prior fatty-bone-marrow space and where there is no volume limit as at periosteal surfaces - occurs as non-scaffolded tissue, locally remote from existing bone surfaces, making it unlikely that 'signalling' occurs from bone cells as such. Further, we question whether the most important 'bone-lining-cell' might not be the adipocyte.

Maintenance of exercise inhibits resorption: withdrawal leads to a catch-up phase in which it is markedly increased, seen in both dense cortical bone and in the number of cutting cones invading ACC, here weakening the osteochondral junction.

Overwork in bone and ACC leading to incipient cracking is repaired by intercalation of a high-density-mineralised-infill (HDMI) material screaming for widespread recognition. It squirts into hyaline articular cartilage (HAC) to become HDM protrusions (HDMI). These, and fragments of fractured ACC and dead, hypermineralised bone, act as a cutting and grinding paste in the mechanical destruction of HAC in OA.

S2.1

Recent advances and gaps in primary bone cancer: challenges and opportunities

Dr Nathalie Gaspar

Paris, France

Summary

Awaiting summary

S2.2

Bone cancer-associated pain (across the different fields)

Professor Anne-Marie Heegaard

Copenhagen, Denmark

Summary

Awaiting summary

S3.1

Inflammaging and nutrition

Professor Philip Calder

Southampton, UK

Summary

Awaiting summary

S3.2

Bone damage and inflammation: Unravelling their relationship at the molecular level

Dr Amy Naylor

Birmingham, UK

Summary

Arthritic inflammation causes damage to bone, but there is wide variability in the degree of damage seen between arthritis types and between patients with the same diagnosis. The reasons for this are not understood and there are no treatments that target this aspect of disease.

Current treatments for inflammatory arthritis all target components of the immune system but my research, and that of my colleagues at the University of Birmingham and elsewhere, has shown that stromal cells (including synovial fibroblasts) play a major role in controlling both inflammation and damage in arthritis in mice (1,2) and humans (3). Through direct injection of synovial fibroblasts into inflamed arthritic joints (K/BxN serum transfer arthritis) in mice, we demonstrated for the first time that lining layer and sublining fibroblasts have different pathogenic effects – broadly, lining layer fibroblasts drive damage, whilst sublining layer fibroblasts drive inflammation (2).

Our previous work has identified multiple sublining layer fibroblast subsets, with variable expression of key markers, seemingly dependant on their microenvironment/niche and the presence or absence of inflammation (1,4). Understanding the function of these marker proteins is crucial to interpreting their function and the function of the subsets that express them. In this talk I will describe our efforts to understand the role of some of these stromal cell markers and the challenges of unpicking their roles in homeostasis (e.g., bone formation and remodelling), compared to their roles in inflammation. I will show data that provide further evidence that inflammation and bone damage are not directly proportionate and that synovial fibroblasts have a key role to play in controlling bone damage during inflammatory arthritis. Our work to understand the molecular mechanisms that underpin stromal cell control of inflammation and damage aims to identify druggable therapeutic targets that will improve outcomes for patients with erosive disease.

This work is supported by a Career Development Fellowship from Versus Arthritis #21743

1. Croft AP, Naylor AJ, Marshall JL, Hardie DL, Zimmermann B, Turner J, et al. Rheumatoid synovial fibroblasts differentiate into distinct subsets in the presence of cytokines and cartilage. Arthritis Res Ther. 2016 Dec 18;18(1):270.
2. Croft AP, Campos J, Jansen K, Turner JD, Marshall J, Attar M, et al. Distinct fibroblast subsets drive inflammation and damage in arthritis. Nature. 2019 Jun 29;570(7760):246–51.
3. Mizoguchi F, Slowikowski K, Wei K, Marshall JL, Rao DA, Chang SK, et al. Functionally distinct disease-associated fibroblast subsets in rheumatoid arthritis. Nat Commun. 2018 Feb 23;9(1):789.
4. Choi IY, Karpus ON, Turner JD, Hardie D, Marshall JL, de Hair MJH, et al. Stromal cell markers are differentially expressed in the synovial tissue of patients with early arthritis. PLoS One. 2017 Aug 9;12(8):e0182751.

S4.1

Rapid-throughput skeletal phenotyping of 1000 knockout mice identifies new target genes in bone and cartilage

Professor Duncan Bassett

London, UK

Summary

The International Mouse Phenotyping Consortium (IMPC) is generating knockout mouse lines for each of the ~24,000 protein coding genes with the aim of deciphering the function of all genes encoded by the mammalian genome. The International Mouse Phenotyping Resource of Standardised Screens (IMPRESS) reports a primary phenotype that includes 233 variables from 28 physiological systems for each of these knockout lines. However, the IMPReSS skeletal screen, which comprises a plain X-ray and a DEXA scan, lacks sensitivity and functional data. Accordingly, the Wellcome Trust funded The Origins of Bone and Cartilage Disease Programme (OBCD) at Imperial College and The Garvan Institute to enhance the IMPC primary screen to identify biologically significant and functionally relevant skeletal phenotypes in mice generated at the Wellcome Trust Sanger Centre for the IMPC. OBCD developed rapid-throughput bone and joint phenotyping pipelines to analyse these samples. The OBCD bone pipeline assesses both long bones and vertebrae, reports 19 structural and strength parameters, and determines bone quality. Parameters are compared to wild type reference ranges determined using more than 400 age, sex, and genetic background matched samples from the same animal facility. To date, the OBCD bone pipeline has phenotyped 1017 unselected knockout mouse lines of which 301 (30%) have at least one outlier skeletal parameter. These studies have already identified many genes not previously known to have a role in bone and cartilage and have been critical in the functional annotation of recent skeletal GWAS and transcriptomic studies.

S4.2

Genetic regulation of human bone mass

Professor Emma Duncan

London, UK

Summary

Awaiting summary

S5.1

Romosozumab or Teriparatide for Severe Osteoporosis?

Professor Stuart Ralston

Edinburgh, UK

Summary

Awaiting summary

S5.2

What is the future for Bisphosphonates?

Professor Graham Russell

Oxford, UK

Summary

Bisphosphonates continue to be the major drugs used worldwide as inhibitors of bone resorption in Paget's disease, osteoporosis, bone oncology and several other skeletal disorders. We first described their biological and pharmacological effects over 50 years ago (1). The pharmacological effects of BPs as inhibitors of bone resorption appear to depend upon two key properties: their affinity for bone mineral, and their inhibitory effects on osteoclasts (2, 3), mediated in the case of the so-called nitrogen-containing BPs by inhibition of the enzyme farnesyl diphosphate synthase in the mevalonate pathway for cholesterol biosynthesis. This in turn reduces the prenylation of multiple GTP binding proteins involved in intracellular signaling.

Many recent studies suggest that BPs may have other clinical benefits beyond their utility in bone diseases. The most intriguing of these are possible reductions in mortality, most convincingly seen in two placebo-controlled trials with zoledronate (4).

Multiple observational studies have revealed an array of positive effects not only on life span (5), but also on many other conditions, including cardiovascular disease, colon and other cancers, diabetes, hearing loss, and pulmonary infections, including large effects on Covid-19 (6).

Are there plausible explanations for these pleotropic effects? BPs can access non-mineralised tissues (7). The extensive range of currently reported non-skeletal effects include extending longevity in mouse models of progeria (8), enhancing human stem cell life span, DNA repair and tissue regeneration (9), effects on tumour growth, prevention of oxidative damage, promotion of autophagy (10), and modulation of cellular senescence (11).

In summary BPs have proved to be not only highly effective but also generally very safe drugs for skeletal diseases. There are obvious opportunities for extending the use of BPs to other areas of medicine, especially multimorbidity in the elderly. In addition, BPs are now being evaluated for their ability to target drugs to bone for local release (12).

Selected references

1. R. G. Russell, Bisphosphonates: the first 40 years. Bone 49, 2-19 (2011).
2. F. H. Ebetino et al., Bisphosphonates: The role of chemistry in understanding their biological actions and structure-activity relationships, and new directions for their therapeutic use. Bone 156, 116289 (2022).
3. S. Cremers, M. T. Drake, F. H. Ebetino, J. P. Bilezikian, R. G. G. Russell, Pharmacology of bisphosphonates. Br J Clin Pharmacol 85, 1052-1062 (2019).
4. I. R. Reid et al., Zoledronate. Bone 137, 115390 (2020).
5. J. R. Center, K. W. Lyles, D. Bliuc, Bisphosphonates and lifespan. Bone 141, 115566 (2020).
6. J. Thompson et al., 10.1101/2022.06.14.22276397 (2022).

7. H. M. Weiss et al., Biodistribution and plasma protein binding of zoledronic acid. Drug metabolism and disposition: the biological fate of chemicals 36, 2043-2049 (2008).
8. I. Varela et al., Combined treatment with statins and aminobisphosphonates extends longevity in a mouse model of human premature aging. Nat Med 14, 767-772 (2008).
9. J. Misra et al., Zoledronate Attenuates Accumulation of DNA Damage in Mesenchymal Stem Cells and Protects Their Function. Stem Cells 34, 756-767 (2016).
10. P. Jiang et al., Anti-cancer effects of nitrogen-containing bisphosphonates on human cancer cells. Oncotarget 7, 57932-57942 (2016).
11. P. Samakkarnthai et al., In vitro and in vivo effects of zoledronate on senescence and senescence-associated secretory phenotype markers. bioRxiv 10.1101/2023.02.23.529777 (2023).
12. S. Sun et al., Bisphosphonates for delivering drugs to bone. British Journal of Pharmacology 10.1111/bph.15251 (2021).

S6.1

A cellular atlas of human MSK tissues: opportunities and insights for the future

Professor Jennifer Westendorf

USA

Summary

Awaiting summary

S6.2

Zebrafish models for studies of musculoskeletal tissues

Dr Chrissy Hammond

Bristol, UK

Summary

Awaiting summary

Oral Presentation Abstracts

Cancer and Bone Workshop Oral Presentations

P001

Characterisation of osteosarcoma cell matrix signatures reveals nanoscale molecular composition is linked to pro-angiogenic potential.

Aikta Sharma[1], Richard Oreffo[2], Sumeet Mahajan[3], Stephen Beers[4], Janos Kanczler[2], Claire Clarkin[5]
[1]University College London, Mechanical Engineering, London, United Kingdom
[2]University of Southampton, Institute of Developmental Sciences, Southampton, United Kingdom
[3]University of Southampton, Chemistry, Southampton, United Kingdom
[4]University of Southampton, Cancer Sciences, Southampton, United Kingdom
[5]University of Southampton, Biological Sciences, Southampton, United Kingdom

Abstract Text

Background. A defining feature of osteosarcoma (OS) is the synthesis of a pathological extracellular matrix (ECM) that is accompanied by a dedicated tumour vascular network, both of which critically support metastatic progression. This study focused on determining whether the ECM signatures OS cell lines are distinct from osteoblasts (OBs) by grade, and whether cell-specific matrices couple to angiogenic potential.

Methods. OS cell lines, Saos-2 (low-metastatic grade) and 143B, (high-metastatic grade) were cultured for up to 14 days *in vitro*. Raman spectroscopy was performed on individual OS cells (N=25) to characterise OS-ECM composition and compared to OB-ECM (MC3T3) signatures. Angiogenic and osteogenic differentiation status was performed in parallel by quantification of VEGF release by ELISA and enzymatic alkaline phosphatase (ALP) assays, respectively.

Results. Raman spectroscopy revealed elevations in collagen-specific proline of the OS-ECM were exclusive to 143B cultures (P=0.007) on day 14, versus MC3T3s. Grade-specific distinctions in immature (amorphous calcium phosphate, ACP) and mature (carbonated apatite, CAP) precursors of hydroxyapatite were evident with low ACP (day 1 and day 4, P<0.0001; day 14, P=0.04) and high CAP (day 1, day 4 and day 14, P<0.0001) in Saos-2 cultures and high ACP (day 4 and day 14, P<0.0001) and low CAP (day 1, day 4 and day 14, P<0.0001) in 143B cultures versus MC3T3s. This correlated with elevated ALP activity in Saos-2 cultures across all time-points (day 1, P=0.0001; day 4 and day 14, P<0.0001) versus MC3T3s. VEGF release was elevated on day 1 (P=0.001) in Saos-2 cultures and day 4 (P<0.0001) and on day 14 in 143B cultures (P<0.0001) versus MC3T3s.

Conclusions. The ECM signatures of OS are distinguishable from OBs by grade and linked to distinct angiogenic and osteogenic differentiation profiles. Our data suggests that such ECM signatures can be used to report metastatic potential in a diagnostic and prognostic capacity.

P002

Oestrogen has a protective effect on chondrosarcoma growth in vitro and in vivo

Karan Shah[1], *Dionne Wortley*[2], *Lee Jeys*[2], *Alison Gartland*[1]
[1]*The University of Sheffield, Oncology and Metabolism, Sheffield, United Kingdom*
[2]*Royal Orthopaedic Hospital, Knowledge Hub, Birmingham, United Kingdom*

Abstract Text

Chondrosarcoma is the most common primary bone cancer (PBC) in adults and is responsible for greatest number of new cases of PBC. Relatively little is known about the aetiology of chondrosarcoma nor why a low-grade tumour de-differentiates, greatly reducing the 5-year survival rate to 29%. Chondrosarcoma affects men more than women (ratio1.5:1) and recent clinical data suggests that women have improved survival compared to men of comparable age. This effect diminishes after menopause, suggesting that oestrogen may have a protective effect in chondrosarcoma. In this study, we investigate the effects of oestrogen on human SW1353 chondrosarcoma cell proliferation and migration *in vitro* and on tumour growth *in vivo*.

The *in vitro* experiments were performed in oestrogen deplete conditions with exogenous oestrogen supplemented at varying concentrations (0-500nM). Cell proliferation was measured following oestrogen treatment for 72hr using WST-1 reagent and cell migration was assessed over 24hr using 'scratch' assays. SW1353 cell proliferation was 80% lower in oestrogen containing culture conditions compared to deplete conditions ($P<0.0001$) and addition of exogenous oestrogen (>10nM) to the deplete conditions lowered cell proliferation by 21% ($P<0.05$). Oestrogen reduced SW1353 cell migration in a dose-dependent manner with significant reduction observed for doses of 10nM and above ($P<0.05$).

For the *in vivo* study, 7-week old female NOD-scid gamma mice were subjected to ovariectomy (OVX), to mimic post-menopausal status, or sham-operated. One week post-surgeries, mice were injected with $2.5x10^5$ luciferase-expressing SW1353 cells sub-cutaneously and tumour burden monitored via bioluminescence imaging. At day 31, higher tumour burden was observed in the OVX mice compared to the sham controls ($1.53x10^6$ vs $6.76x10^5$; $P<0.0001$).

These preliminary data indicate that oestrogen plays a protective role in the progression of chondrosarcoma and are consistent with the clinical findings. A more comprehensive investigation is warranted to test the therapeutic potential of oestrogen supplementation in chondrosarcoma.

P003

Evidence for altered osteocyte morphology proximal to myeloma bone disease using synchrotron radiation micro-CT imaging

Rebecca Andrews[1], *Holly Evans*[1], *Jacob Trend*[2], *Goran Lovric*[3], *Claire Clarkin*[2], *Michelle Lawson*[1]
[1]*University of Sheffield, Oncology and Metabolism, Sheffield, United Kingdom*
[2]*University of Southampton, Developmental and Skeletal Biology, Southampton, United Kingdom*
[3]*Paul Scherrer Institut, Photon Science Division, Villigen, Switzerland*

Abstract Text

Myeloma is a blood cancer in which up to 90% of patients develop bone disease, resulting in osteolytic lesions, reduced bone mineral density and trabecular thinning. These changes cause pain, immobility, and risk of fracture. The impact on quality of life for patients is significant and there is an unmet clinical need to develop better treatments. Historically, it has not been possible to properly assess or quantify osteocyte lacunae, as its visualisation requires sub-micron resolution. Recently we acquired access to the Swiss Light Source (Paul Scherrer Institute, Switzerland) to obtain high-resolution synchrotron radiation micro-CT images of long bones from mice with myeloma bone disease (MBD) and controls. We hypothesised that osteocyte lacunae are significantly altered in myeloma-bearing bones compared to non-tumour controls, potentially contributing to bone destruction. We scanned long bones of both synergic (5TGM1) and xenograft (U266) models of myeloma at a resolution of 0.65um², allowing us to visualise osteocyte lacunae using Dragonfly. By comparing tumour mice to naïve controls, we were able to show that osteocyte parameters remained similar at the tibiofibular junction, a region far from osteolytic disease – osteocyte density was 56816 ± 5429/mm³ in diseased bone vs 58819 ± 9190/mm³ in naïve bone; and average osteocyte volume was 110.1 ± 12.0 um³ vs 172.0 ± 122.2um³. However, in a region close to osteolytic disease at the growthplate, we showed that osteocyte density decreased but volume increased – osteocyte density was 6143 ± 1231/mm³ in diseased bone vs 14346 ± 2417/mm³ in naïve bone; osteocyte volume was 385.5 ± 31.2um³ vs 185.8 ± 12.1mm³. In summary, we observed changes in the density and volume of osteocyte lacunae in areas of established osteolytic lesions compared to non-MBD regions, raising questions as to the role of osteocytes in myeloma and the potential for them to be targeted therapeutically.

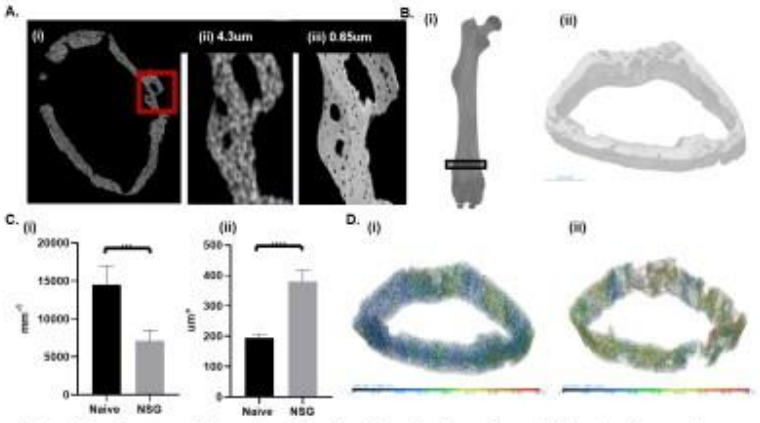

Figure 1. Synchrotron radiation micro-CT imaging of myeloma bone disease. (A) Imaging of a mouse femur, with (i) a cross-sectional image with the red highlighted region then scanned on (ii) a benchtop micro-CT scanner at 4.3μm and (iii) using synchrotron radiation micro-CT (SRCT) at 0.65μm. (B) 3-d rendering of of (i) scanned femur and (ii) the region analysed (C) Femoral analysis in naïve and NSG mice of (i) osteocyte density and (ii) osteocyte volume. (D) Representative 3-D images showing osteocyte volume for (i) naïve and (ii) NSG mice.

P004

Monitoring breast cancer-induced bone disease in nude mice using in vivo µCT

Yue Chun Jacky Wong[1], Lubaid Saleh[2], Holly R. Evans[2], Enrico Dall'Ara[3], Michelle A. Lawson[2], Ingunn Holen[2]
[1]Univesity of Sheffield, Oncology and metabolism, Sheffield, China
[2]University of Sheffield, Oncology and metabolism, Sheffield, United Kingdom
[3]University of Sheffield - INSIGNEO Institute for in silico Medicine, Oncology and metabolism, Sheffield, United Kingdom

Abstract Text

Background: Breast cancer-induced bone disease is a result of localised lytic bone lesions that cause bone fragility and pain. Previous studies have mainly used *ex vivo* µCT to investigate the end-stage effects of breast tumour growth in bone. We investigated whether *in vivo* µCT, combined with bioluminescence imaging of tumour burden, can be used to detect the formation and map the development of breast cancer-induced bone lesions in nude mice.

Methods: 6-week-old female BALB/c nude mice were injected (intra cardiac) with $5x10^5$ Luc2+ve MDA-MB-231 cells (n=10). Tumour growth was monitored by bioluminescence imaging twice weekly, left proximal tibiae and distal femora were scanned by *in vivo* µCT once weekly (VivaCT80 µCT scanner) and by *ex vivo* µCT at endpoint.

Results: Tumours developed in hind limbs of all mice by week 2 after tumour injection, with tumour burden increasing up to 4 weeks. No soft tissue tumour growth was detected. *In vivo* µCT demonstrated that lytic lesions appeared in the tibia 1 week after tumour injection and in the femur after 3 weeks, with large lesions established in either the tibia or the femur after 4 weeks. In both tibia and femur, trabecular BV/TV (%), trabecular number (mm^{-1}) and trabecular thickness (mm) were decreased 1 week after tumour injection compared to baseline, this decrease continued over the following 3 weeks (Table 1). *Ex vivo* µCT results (BV/TV (%)) agreed with the *in vivo* µCT results at week 4. Taken together, trabecular BV/TV (%) decreased as tumour burden increased.

Conclusion: Our results support that *in vivo* µCT can be used to track the development of lytic bone lesions from the very early stages of breast cancer-induced bone disease.

Table 1. Left hindlimb bone parameters detected by weekly *in vivo* µCT

	Percentage bone volume (BV/TV)		Trabecular thickness (Tb.th)		Trabecular number (Tb.N)	
	Tibia					
Week	Mean	*P*	Mean	*P*	Mean	*P*
0	4.651		0.034		4.55	
1	4.226	*,0.0137	0.032	0.4646	2.181	****,<0.0001
2	3.443	****,<0.0001	0.027	****,<0.0001	1.27	****,<0.0001
3	2.14	****,<0.0001	0.028	****,<0.0001	0.654	****,<0.0001
4	1.693	****,<0.0001	0.025	****,<0.0001	0.42	****,<0.0001
	Femur					
Week	Mean	*P*	Mean	*P*	Mean	*P*
0	6.076		0.034		2.456	
1	5.328	****,<0.0001	0.032	0.4646	2.42	0.9932
2	4.626	****,<0.0001	0.027	****,<0.0001	1.433	****,<0.0001
3	4.014	****,<0.0001	0.028	****,<0.0001	1.144	****,<0.0001
4	3.135	****,<0.0001	0.025	****,<0.0001	0.816	****,<0.0001

& ** significant compared to week 0 baseline (before tumour cell injection)*

P005

Targeting dormant myeloma cells using standard of care therapies

Hawazen Algifry[1], Georgia Stewart[2], Darren Lath[1], Jennifer Down[1], Alexandria Sprules[1], Munitta Muthana[1], Michelle Lawson[1]
[1]University of Sheffield, Oncology & Metabolism, Sheffield, United Kingdom
[2]University of Sheffield, Oncology and Metabolism, Sheffield, United Kingdom

Abstract Text

Background: Multiple myeloma is caused by abnormal plasma cell growth in the bone marrow and disease reoccurrence post chemotherapy is common. It has been speculated that dormant myeloma cells (DMCs) that residue in endosteal bone niches play a role in disease relapse due to their drug resistance. Therefore, we aimed to assess the efficacy of standard of care (SoC) anti-myeloma therapies on DMCs. We hypothesise SoC anti-myeloma therapies when used in combination can target DMCs more effectively than single therapies.

Methods: Four myeloma cell lines (murine 5TGM1, and human JJN3, OPM2, U266 transduced with GFP and Luc) were labelled with a vybrant membrane dye 1,1'-dioctadecyl-3,3,3',3'-tetramethylindodicarbocyanine (DID) to track DMCs over 21 days of culture using fluorescent microscopy and flow cytometry. Cell populations were treated with different concentrations of SoC therapies (bortezomib, melphalan, and panobinostat) to determine IC_{50} values on cell viability after 3 and 5 days of culture using an alamarBlue™ asssay.

Results: Fluorescent microscopy and flow cytometry demonstrated the presence of DID-labelled cells (DID^{high}: potential DMCs, DID^{low}: slow growing MCs, and $DID^{negative}$: proliferating cells) and these declined over time in all cell lines. DID^{high} cells were observed in 5TGM1 (0.1%) and JJN3 (0.2%) cultures at 17 days, by day 21 <0.1% DID^{high} cells were detected. For OPM2 cells, no DID^{high} cells were detected after 10 days. The IC_{50} values of SoC therapies were determined (bortezomib 0.58-1.93nm, melphalan 0.54-4.98nm, and panobinostat 0.36-13.37nm).

Conclusions: In summary, we have demonstrated for the first time the presence of DMCs in cultures JJN3 cells. We have determined drug IC50 values in 4 cell lines and these will be used in future *in vitro* and *in vivo* studies to determine their efficacy on DMCs when used alone or in combination.

Muscle and Bone Workshop Oral Presentations

P302

Low muscle density in children with osteogenesis imperfecta using low-dose chest CT: a case-control study

Yi Yuan[1], Wenshuang Zhang[1], Ling Wang[1], Xiaoguang Cheng[1]
[1]Peking University Fourth School of Clinical Medicine- Beijing Jishuitan Hospital, Department of Radiology, Beijing, China

Abstract Text

Introduction: Low-dose chest computed tomography (CT) can be used to measure muscle size (cross-sectional area) and muscle density (mean Hounsfield Units [HU]) of the trunk muscles. It is essential to develop a better understanding of the muscle differences in osteogenesis imperfecta (OI) children.
Purpose: The aim of the present study was to investigate the muscle differences in OI children using low-dose chest CT.
Materials and methods: This retrospective study was approved by institutional review board. A total of 20 OI children (3-14years; 15 males) and 40 age- and sex-matched controls were enrolled. 60 children were performed low-dose chest CT for other clinical indications. From the CT images, muscle size and muscle density of the trunk muscles were measured on 1 slice each at the mid-T4 and the mid-T10 level. The intraclass correlation coefficients (ICC) were calculated to evaluate interobserver and intraobserver variability. Muscle differences were analyzed with Student *t* tests and Mann-Whitney *U* tests.
Results: Interobserver agreement were excellent (ICC, 0.981-0.994) and intraobserver agreement were excellent (ICC, 0.981-0.995). Compared with control group, OI children had lower T4 muscle density (P<0.001) but normal muscle size (P=0.132). They also had lower T10 muscle density (P<0.001) than control group but normal muscle size (P=0.071). Moreover, children under 10 years old had significantly smaller T4 and T10 muscle size than beyond 10 years old in OI children (all P<0.001). However, children under 10 years old had significantly higher T4 and T10 muscle density than beyond 10 years old in OI children (P=0.029, 0.004, respectively).
Conclusion: These results suggested that muscle density may represent a more clinically meaningful indication of muscle performance than muscle size in OI children. Muscle density can be easily obtained from low-dose chest CT. Therefore, muscle density may have the potential to lead to novel therapeutic approaches.

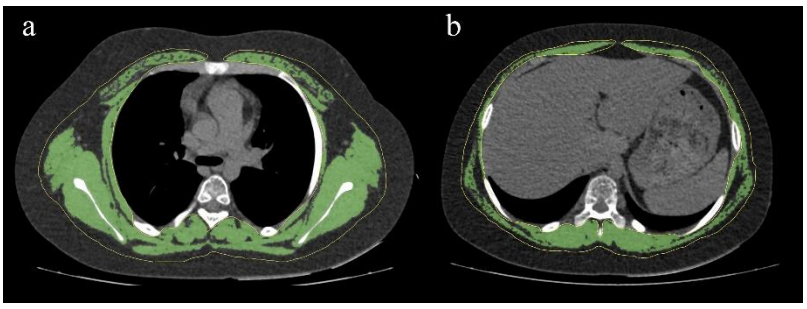

P165

Change in musculoskeletal hypermobility in adolescents between the ages of 14 and 17 in the Avon Longitudinal Study of Parents and Children (ALSPAC)

Clare Shere[1], *Emma M Clark*[1], *Shea Palmer*[2]
[1]*University of Bristol, Musculoskeletal Research Unit, Bristol, United Kingdom*
[2]*Coventry University, Centre for Care Excellence, Coventry, United Kingdom*

Abstract Text

Background

Musculoskeletal hypermobility is a common trait in the population. It can exist as part of heritable syndromes such as Ehlers-Danlos syndrome, or in isolation on a spectrum. It is thought to reduce with age. Although generally asymptomatic, at extremes individuals can experience joint clicking and musculoskeletal pain.

Aim

To investigate how musculoskeletal hypermobility changes between age 14 and 17 in adolescents in the Avon Longitudinal Study of Parents and Children (ALSPAC).

Methods

Musculoskeletal hypermobility was measured using the Beighton score in individuals aged 14 and aged 17 years in ALSPAC. Complete data was available for 3972 individuals (2184 females, 1788 males). We have described the change in prevalence of musculoskeletal hypermobility as defined by Beighton score ≥6 out of 9. We performed logistic regression to look for predictors of hypermobility stability, gain or loss from aged 14 to 17.

Results

The prevalence of generalised musculoskeletal hypermobility remained stable between aged 14 and 17, at 4.6%. The most common area of musculoskeletal hypermobility was in the fingers (42.2% aged 14 and 27.6% aged 17). The odds of being hypermobile at aged 14 were 4.8x higher in females compared with males, and 2.5x higher aged 17 in females compared with males. Being hypermobile at the wrists/thumbs aged 14 most strongly predicted generalised hypermobility aged 17 (OR 7.4 (95% CI 6.2, 8.9)). Despite overall stable prevalence of hypermobility between aged 14 and aged 17, there was considerable change in hypermobility between individuals, with some becoming hypermobile and some losing hypermobility. We identified no association between BMI, pubertal stage or physical activity and hypermobility stability, gain or loss.

Conclusions

This novel analysis shows prevalence of hypermobility is unchanged across adolescence. Wrist/thumb hypermobility could predict future generalised hypermobility. Further investigation may elucidate

predictors of hypermobility gain or loss during adolescence.

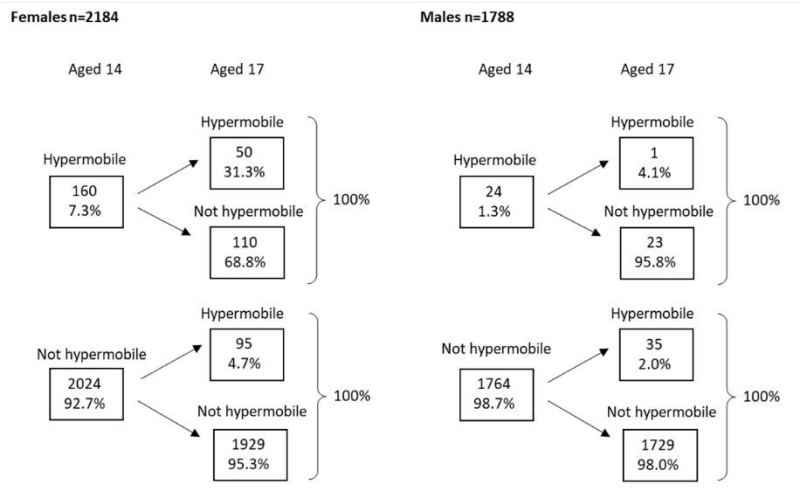

P193

Process evaluation of elastic resistance band training to benefit vertebral fracture risk in postmenopausal women

Donghyeon Seo[1], Amelia Morgan[1], Fehmidah Munir[1], Daniel T. P. Fong[1], Michelle Hui[2], Katherine Brooke-Wavell[1]
[1]Loughborough University, School of Sport- Exercise and Health Sciences, Loughborough, United Kingdom
[2]University Hospitals of Derby and Burton NHS Foundation Trust, Department of Rheumatology, Derby, United Kingdom

Abstract Text

Background: Progressive resistance training could reduce vertebral fracture risk by increasing bone and muscle strength and reducing kyphosis or fall risk. Elastic resistance bands (ERB) may be a feasible and attractive mode, but efficacy and acceptability are unknown.

Purpose: To examine the adherence, acceptability, satisfaction, and efficacy of an ERB training programme in postmenopausal women.

Methods: A randomised-controlled trial was conducted in 41 women aged 60-80 approved by National Research Ethics Service. One group and two home ERB sessions were prescribed each week, with regular progression of band stiffness. Bone mineral density (BMD) and Cobb angle were assessed by dual X-ray absorptiometry; back extensor strength by dynamometer; endurance by time maintaining back extension and dynamic balance by timed-up and go (TUG). Participant views of the intervention were explored by questionnaire at the end of the study.

Results: 88% of exercisers and 75% of controls completed the study. Exercisers attended 83% of group sessions and 84% of home sessions. Missed sessions were mostly due to holiday, illness and caring responsibilities. Social contact, regular time slot, supervision and exercise log facilitated adherence. Motivators included helping research and improving health. Reported advantages of ERB were their portability, simplicity and possibility for progression but disadvantages were boredom and bands snapping. Most exercisers (but not controls) perceived benefits to strength, energy, posture, balance and confidence to exercise. BMD did not change in exercisers versus controls but there were benefits to Cobb angle (-4.6 vs +5.4%, $p<0.01$), back extensor strength (+15.3% vs +2.5%, $P=0.05$), endurance (+38.5% vs -3.1%, $p<0.01$) and TUG (-10.4% vs -3.1%, $p=0.02$).

Conclusions: The ERB programme was feasible and acceptable. Short duration and small sample size may have limited power to detect BMD change. The programme may improve back extensor strength, posture and dynamic balance, and hence reduce the risk of vertebral fractures.

Rare Bone Diseases Workshop Oral Presentations

P099

FGFR2 mutation disturbs bone repair and formation in a mouse model of Crouzon syndrome

Anne Morice[1], Amélie De La Seiglière[1]
[1]Imagine Institute, Laboratory of Molecular and Physiopathological Bases of Osteochondrodysplasia, Paris, France

Abstract Text

Fibroblast growth factor receptor 2 (FGFR2) mutations are responsible for syndromic craniosynostoses, among them Crouzon syndrome is the most frequent. Patients present coronal craniosynostoses, midface hypoplasia and proptosis. Patients often require maxillomandibular osteotomies to restore normal dental occlusion and facial contours. Recently, the impact of the mutation has been reported during bone growth in patients with FGFR2 craniosynostoses. The role of FGFR2 in calvaria is well described, the activation of FGFR2 receptor induces premature fusion of the coronal sutures. Despite the previous findings, to date, there are no reported research that directly implicates FGFR2 activation in mandible bone repair and bone formation. Here, we performed experiments using the Crouzon mouse model *Fgfr2*$^{C342Y/+}$ mimicking human pathology. We generated non-stabilized mandibular fractures and analysed the calluses from 14 to 28 days post fracture (end of the consolidation period). MicroCTscan analyses showed a significant increase of the BV/TV (+7.15 %; $p<0.01$) in *Fgfr2*$^{C342Y/+}$ calluses compared to the controls (day 28 post fracture), highlighting increased bone mineralization of the bone calluses in *Fgfr2*$^{C342Y/+}$ mice. Our histomorphometric analyses showed no significant impact of *Fgfr2*$^{C342Y/+}$ on chondrocyte proliferation and differentiation, showing that *Fgfr2*$^{C342Y/+}$ mutation preferentially disturbs the osteoblastic lineage. Although bone mineralization was increased in *Fgfr2*$^{C342Y/+}$ mice, we observed no significant acceleration of bone callus remodeling. Finally, we analyzed the axial and appendicular skeleton, we showed a significant decrease of the naso-anal length (-6.2%; $p<0.05$) and a reduced length of the tibia (-2.93%; $p<0.05$) at P21 in *Fgfr2*$^{C342Y/+}$ mice. Altogether, we demonstrate that *FGFR2*, mainly expressed in osteoblasts, controls the bone elongation and bone repair process. In the future this better understanding of the impact of *FGFR2* activating mutations on bone growth and repair will allow a better surgeon and physician care.

P331

Conditional knockout of renal homogentisate dioxygenase to assess the role of the kidney in homogentisic acid metabolism for future genetic therapies of alkaptonuria

Dominic Rutland[1], *Brendan P Norman*[1], *Peter JM Wilson*[1], *Hazel Sutherland*[1], *Lakshminarayan R Ranganath*[1], *James A Gallagher*[1], *George Bou-Gharios*[1]
[1]*University of Liverpool, Institute of Life Course and Medical Sciences, Liverpool, United Kingdom*

Abstract Text

Background

Alkaptonuria (AKU), known as black bone disease, is a recessive disorder caused by a deficiency of functional homogentisate dioxygenase (HGD) enzyme. The loss of HGD activity causes homogentisic acid (HGA) to accumulate in the plasma and urine, resulting in severe early-onset osteoarthropathy. Ordinarily, HGD is expressed in the liver and proximal tubules of the kidney. Current treatment for AKU involves inhibiting the production of HGA, which causes tyrosinaemia; this treatment is therefore not a cure, and the future of AKU treatment will involve gene therapy.

Purpose

To examine the contribution of the kidney to maintain physiological plasma and urine HGA concentrations through a kidney-specific knockout of HGD in mice.

Methods

Kidney-specific HGD knockout was performed using a conditional knockout model, which allows the removal of *Hgd* exon 6 using inducible Cre recombinase, thereby disrupting HGD expression. *Pax8-CreER^{T2}* is used to allow for kidney-specific recombination with a temporal control, so gene recombination will only take place upon the administration of tamoxifen.

Results

Following tamoxifen injection, DNA extracted from the kidney of *Pax8-CreER^{T2}* mice showed the presence of a 700bp PCR product of the recombined *Hgd* gene. The 700bp band was not seen in mice not carrying the *Pax8-CreER^{T2}* gene, and no 700bp product was observed in liver extracts from either Cre or non-Cre mice, confirming *Hgd* recombination is limited to the kidney only. LC-MS analysis of urine samples collected showed an increase in urine HGA concentration of *Pax8-CreER^{T2}* mice after tamoxifen administration, but no such increase in non-Cre mice, along with no increase in plasma HGA for both *Pax8-CreER^{T2}* and non-Cre mice.

Conclusions

Partial knockout of up to 40% kidney HGD resulted in increased urinary HGA concentration, with no observable effect on circulating HGA. Future studies will aim to achieve full kidney HGD knockout to definitively establish the necessity for repairing kidney HGD expression in future AKU gene therapies.

A

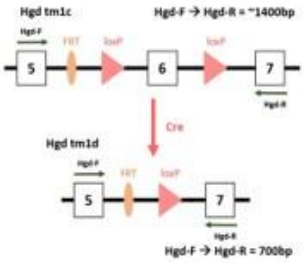

(a) Schematic of *Hgd tm1c* (*Hgd* conditional knockout model) gene and the result of Cre recombination to knockout HGD expression. Diagram shows location of binding sites for primers (*Hgd-F* and *Hgd-R*) to assess recombination of *Hgd tm1c*, and anticipated length of PCR product for both pre- and post-Cre recombination. (b) Gel electrophoresis of post-tamoxifen DNA extracts to identify Cre recombination of *Hgd* gene. DNA extracted from kidney and liver tissues of both *Pax8-CreER*^{T2} and non-Cre mice. Positive signal for recombination (700bp band) observed in *Pax8-CreER*^{T2} kidney extract, but in no other tissues. ~1400bp band observed in all tissues shows the presence of intact *Hgd* tm1c. (c) LC-MS analysis of urine collected from both *Pax8-CreER*^{T2} and non-Cre, before and after tamoxifen administration. Pre-tamoxifen, HGA concentration below level of quantification (LOQ) for both *Pax8-CreER*^{T2} and non-Cre mice. Post-tamoxifen, HGA concentration increased in *Pax8-CreER*^{T2} mice, but no increase detected in non-Cre mice

B

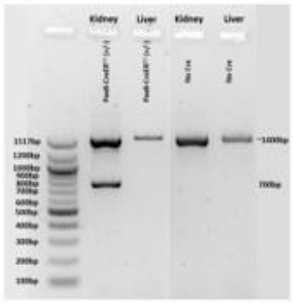

C

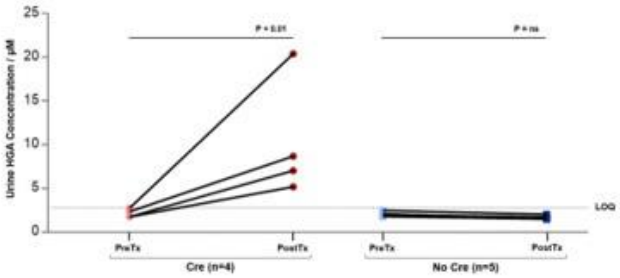

BRS Annual Meeting Oral Presentations

OC1.1

Relative growth rates for height among Zimbabwean children and adolescents living with HIV and established on antiretroviral therapy

Tafadzwa Madanhire[1], Victoria Simms[1], Cynthia Mukwasi-Kahari[2], Nyasha Dzavakwa[2], Farirayi Kowo-Nyakoko[4], Rashida Ferrand[5], Kate Ward[6], Celia Gregson[7], Andrea Rehman[2]
[1]Biomedical Research and Training Institute, Statistics, Harare, Zimbabwe
[2]London School of Hygiene and Tropical Medicine, Infectious Disease Epidemiology, London, United Kingdom
[4]University of Southampton, Global musculoskeletal health, Southampton, United Kingdom
[5]Biomedical Research and Training Institute, Principal Investigator, Harare, Zimbabwe
[6]London School of Hygiene and Tropical Medicine, MRC Unit The Gambia, Banjul, Gambia
[7]University of Bristol, Musculoskeletal Research Unit, Bristol, United Kingdom

Abstract Text

Background: Perinatally acquired HIV is a treatable chronic condition such that through antiretroviral therapy (ART), children with HIV (CWH) are now surviving to adulthood. However, CWH often exhibit impaired growth. We aimed to identify the height growth patterns among CWH and determine age at peak-height-velocity (PHV).

Methods: This is a secondary analysis of data collected prospectively in the ongoing VITALITY randomised controlled trial in Zimbabwe (EDCTP: VITALITY-RIA2018CO-2512). The trial has recruited 422 CWH (11-19 years) established on ART for at least 6 months, to determine whether vitamin-D_3/calcium supplementation improves bone mass and strength with follow-up to 96 weeks. Height is measured at 12-week intervals with currently (15-November-2022) 150 participants having completed 72-weeks of follow-up. Weight and height for age were calculated using 1990-UK-reference values, with Z-score-2 classifying those underweight and stunted. Analysis of height velocity was performed by calculating change in height for each visit by one-year age-band and fitting the mean curve by sex.

Results: We recruited 218(51.7%) females and 204(48.3%) males and followed them up for 0.93(IQR:0.92-1.38) years; at baseline median(IQR) age was 16(13-18) years, 27.7%(n=117) were underweight and 44.5%(n=188) were stunted. CHW were taking ART for median(IQR) 10.1(6.6-12.5) years of their lives and 77.7%(n=328) were on an ART regimen containing tenofovir-disoproxil-fumarate. Lifetime fracture prevalence was 5.5%(n=23). At baseline (n=422), mean(SD) height for age was -2.13(1.06) and -1.74(1.02) for males and females respectively. Over 48-weeks (n=364), median(IQR) height gains were 2.6(1.4-4.9)cm and 1.1(0.8-3.4)cm for males and females separately. Age at PHV was 15.0 years (PHV:6.4cm/year) and 12.5 years (PHV:6.0cm/year) for males and females respectively.

Conclusion: There is a high prevalence of stunting among CWH in Zimbabwe. Both males and females showed delayed PHV compared to regional estimates (females:11.8, males:14.5 years), raising concerns for persistent height deficits in adulthood known to impact human capital and function in later life.

OC1.2

Prenatal exposure to alcohol (PAE) negatively affects the skeleton in male mice

Lucie Bourne[1], Fergus Guppy[2], Victoria Jarvis[1], Rakul Mathavan[1], Paul Gard[1], Nigel Brissett[1], Katherine Staines[1]
[1]University of Brighton, School of Applied Sciences, Brighton, United Kingdom
[2]Heriot Watt University, School of Energy- Geoscience- Infrastructure and Society, Edinburgh, United Kingdom

Abstract Text

Background
Prenatal exposure to alcohol (PAE) can result in foetal alcohol spectrum disorder, characterised by a variety of cognitive and physical impairments. Whilst the effects of PAE on facial dysmorphology and postnatal growth have been investigated in murine models, its effects on the adult skeleton are unknown.

Purpose
Conduct skeletal phenotyping of a murine model of PAE.

Methods
Pregnant C57Bl/6J females received 5% ethanol in their drinking water during gestation. Offspring from control (n=9 male, 9 female) and alcohol exposed (n=11 male, 5 female) dams were sacrificed at 12-weeks of age. Fluid intake between control (water-only) and alcohol-exposed females was unchanged. Skeletal phenotyping was conducted by microCT and histology. All animal studies were conducted in line with the UK Animals Scientific Procedures act 1986 with local ethical approval.

Results
In male mice, PAE significantly reduced trabecular bone parameters (tissue volume, bone volume, bone surface and intersection surface) by ≤40% ($p<0.001$) and reduced bone volume fraction (BV/TV) by 11% ($p=0.038$). Whilst trabecular thickness and separation were unaffected, trabecular number was reduced (10%, $p=0.02$) and pattern factor increased (42%, $p=0.007$). Fractal dimension was also reduced ($p=0.0098$) indicating that trabecular structure and complexity is altered in male PAE mice. However, preliminary analysis suggests that female PAE littermates are protected from these detrimental effects on the skeleton, as no changes in the above bone parameters were observed. Analysis of growth plates revealed significant decreases in total width (10%), and proliferative (12%) and hypertrophic (12%) zones in PAE male mice ($P<0.01$). However, total bone length in both sexes was unaffected.

Conclusions
Thus, data here demonstrate that PAE in male mice has negative effects on the mature skeleton and adds further evidence to indicate that the environment *in utero* impacts skeletal health. In contrast, female littermates appear to be protected, suggesting a potential sexual dimorphism. Ongoing studies are investigating the mechanistic basis for these effects.

OC1.3

Changes in pQCT measured bone density, size and strength in Zimbabwean children with and without HIV over one year: a cohort study

Cynthia Kahari[1,2], *Celia L. Gregson*[3], *Mícheál Ó Breasail*[4], *Ruramayi Rukuni*[5,6], *Tafadzwa Madanhire*[1,5], *Victoria Simms*[1,5], *Joseph Chipanga*[5], *Lynda Stranix-Chibanda*[7], *Lisa K. Micklesfield*[8], *Rashida A. Ferrand*[5,6], *Kate A. Ward*[9,10], *Andrea M. Rehman*[1]

[1]*London School of Hygiene and Tropical Medicine, Department of Infectious Disease Epidemiology, London, United Kingdom*

[2]*Biomedical Research and Training Institute, The Health Research Unit Zimbabwe THRU-ZIM, Harare, Zimbabwe*

[3]*University of Bristol, Musculoskeletal Research Unit- Bristol Medical School, Bristol, United Kingdom*

[4]*University of Bristol, Population Health Sciences- Bristol Medical School, Bristol, United Kingdom*

[5]*Biomedical Research and Training Institute, The Health Research Unit Zimbabwe THRU ZIM, Harare, Zimbabwe*

[6]*London School of Hygiene and Tropical Medicine, Clinical Research Department, London, United Kingdom*

[7]*University of Zimbabwe Faculty of Medicine and Health Sciences, Child and Adolescent Health Unit, Harare, Zimbabwe*

[8]*University of the Witwatersrand, SAMRC/Wits Developmental Pathways for Health Research Unit- Department of Paediatrics- School of Clinical Medicine, Johannesburg, South Africa*

[9]*University of Southampton, MRC Lifecourse Epidemiology Centre, Southampton, United Kingdom*

[10]*London School of Hygiene and Tropical Medicine, MRC Unit The Gambia at London School of Hygiene and Tropical Medicine, Banjul, Gambia*

Abstract Text

***Introduction*:** Understanding adolescent bone accrual may inform approaches to improve skeletal health and reduce future fracture risk.

Purpose: To determine the effect of HIV on bone growth assessed by pQCT and to what extent effects are explained by impaired longitudinal growth.

Methods: Children with HIV (CWH), on ART for ≥2 years, and children without HIV (CWOH), aged 8-16years (n=609), had tibial pQCT scans at 0 and 12 months. Linear regression estimated differences in mean and change in (Δ) pQCT bone density (trabecular and cortical), size (total cross-sectional area [CSA]) and strength (SSI) between CWH and CWOH; adjusting for socio-economic status (SES) and orphanhood and incorporating an interaction term for baseline pubertal status (Tanner 1-2 [pre/early] vs 3-5[mid/late]). Structural equation modelling tested whether baseline height-for-age-Z-scores mediate the effect of HIV on Δbone outcomes.

Results: CWH and CWOH were similar in age. CWH were more likely to be orphans (44% vs 7%), of lower SES (43% vs 27%) and be stunted (30% vs 8%) than CWOH. At baseline and follow up, CWH had lower trabecular density, CSA and SSI than CWOH. After adjustment, bone density and strength increased similarly in CWH and CWOH. CWH in late puberty had greater increases in CSA than CWOH, particularly in males (mean difference [31.3(95%CI -3.1, 65.6)mm^2 in mid/late puberty vs. -2.04(-23.8, 19.7)mm^2 in

pre/early puberty; interaction p-value=0.013]. Height mediated the effect of HIV on Δbone outcomes only in females as follows: indirect pathways from HIV to Δtrabecular density [-1.85(-3.5, -0.2)mg/cm^3], Δcortical density [-2.01(-3.9, -0.01)mg/cm^3], ΔCSA[-2.59(-4.7, -0.5)mm] and ΔSSI[-18.36(-29.6, -7.2) mm^3].

Conclusion: Puberty modifies the effect of HIV on ΔCSA. CWH show bone deficits at baseline but similar bone growth to CWOH (except bone size). Height explains bone growth in females. Investigations of bone growth earlier in life and post-puberty to peak bone mass are needed.

OC2.1

Assessing the Effects of Bone Anabolic Agents in Immunocompromised Mice using repeated weekly in vivo µCT

Yue Chun Jacky Wong[1], *Lubaid Saleh*[2], *Holly R. Evans*[2], *Enrico Dall'Ara*[3], *Ingunn Holen*[2], *Michelle A. Lawson*[2]
[1]*Univesity of Sheffield, Oncology and metabolism, Sheffield, China*
[2]*University of Sheffield, Oncology and metabolism, Sheffield, United Kingdom*
[3]*University of Sheffield - INSIGNEO Institute for in silico Medicine, Oncology and metabolism, Sheffield, United Kingdom*

Abstract Text

Background: TGF-β maintains bone homeostasis through the coupling of osteoblast and osteoclast activity, agents that inhibit TGF-β are reported to increase bone formation. We investigated whether losartan (angiotensin II inhibitor, causing reduction in TGF-β) and SD-208 (TGF-β type-1 kinase inhibitor) have bone anabolic effects in immunocompromised mice detectable overtime using *in vivo* µCT.

Methods: 6-week-old female BALB/c nude mice were treated with 100µl of losartan (100mg/kg), SD-208 (60mg/kg) or 100µl of PBS (vehicle) by oral gavage 5 days per week for 3 weeks (n=4/group). The left tibias of mice were scanned by *in vivo* µCT once weekly, by *ex vivo* µCT after cull, fixed in PFA, decalcified and analysed by bone histomorphometry.

Results: *In vivo* µCT demonstrated that after 1 week of treatment, trabecular BV/TV (%) was significantly increased compared to vehicle in both losartan and SD-208 treated mice; this increase continued following 2 and 3 weeks of treatment (Table1). Trabecular number (mm^{-1}) increased after 1 week of SD-208 treatment and after 2 weeks of losartan treatment compared to vehicle. *Ex vivo* µCT results (BV/TV (%) agreed with the end stage *in vivo* µCT results.

Bone histomorphometry demonstrated that compared to vehicle, losartan increased the number of osteoblasts/mm on endocortical and trabecular bone surfaces (endocortical medial+lateral sides: vehicle 33.697, losartan 47.834, *P=0.0162* and trabecular bone: vehicle 7.759, losartan, 12.206 *P=0.017*), whilst no effect on osteoclast numbers were observed. No significant difference in numbers of osteoblasts or osteoclasts were observed in SD-208 treated mice compared to vehicle.

Conclusion: *In vivo* µCT showed that both agents cause significant bone anabolic effects after only 1 week of treatment, therefore, they could potentially be used for treating lytic bone lesions. This is the first demonstration that losartan has bone anabolic effects in BALB/c nude mice.

Table 1. Tibiae bone parameters using *in vivo* µCT

	Percentage bone volume (BV/TV)		Trabecular thickness (Tb.th)		Trabecular number (Tb.N)	
Weeks	Vehicle					
0	1.4		0.031		0.44	
1	1.64		0.033		0.49	
2	1.91		0.034		0.56	
3	2.19		0.036		0.62	
	SD-208					
Weeks		*P*		*P*		*P*
0	1.54	0.441	0.03	0.175	0.42	0.797
1	2.22	**,0.0439	0.033	0.681	0.67	*,0.0381
2	2.9	****, 0.0002	0.038	*,0.0742	0.77	**,0.0111
3	3.1	****, 0.0008	0.042	*,0.0021	0.79	**,0.0336
	Losartan					
Weeks		*P*		*P*		*P*
0	1.4	0.815	0.034	0.876	0.46	0.562
1	2.77	****,0.0009	0.034	0.113	0.81	0.0676
2	3.31	****,<0.0001	0.035	0.313	0.92	**,0.0232
3	4.99	****,0.0001	0.041	0.0961	1.2	****,0.0026

OC2.2

Is losartan a bone anabolic for myeloma-induced bone disease?- A pilot study.

Georgia Stewart[1], *Holly Evans*[2], *Darren Lath*[2], *Andrew Chantry*[2], *Michelle Lawson*[2]
[1]*University of Sheffield, Oncology and Metabolism, S10 2RX, United Kingdom*
[2]*University of Sheffield, Oncology and Metabolism, Sheffield, United Kingdom*

Abstract Text

Myeloma-induced bone disease (MBD) can lead to bone pain and increased fracture risk. Current antiresorptive treatments do not repair existing bone damage but recently we have shown that inhibiting TGFβ leads to bone repair in MBD murine models. However, there are no specific TGFβ inhibitors clinically available, therefore, we investigated the use of losartan, an FDA approved drug for hypertension, which is known to target the TGFβ pathway and has positive effects on bone. A *in vivo* pilot study was performed to assess whether losartan could prevent MBD alone or when combined with a chemotherapy (melphalan) compared to control mice.

$1x10^6$ JJN-3-GFP-Luc cells were inoculated into 6-8 w/o female NSG mice (I.V) (ethical consent under PP3267943). 4 days after tumour inoculation, mice were randomised into 4 groups- vehicle (100ul PBS O.G & I.P; n=3), melphalan (5mg/kg 2x/wk I.P, n=3); losartan (100mg/kg 5x/wk O.G, n=4) or melphalan combined with losartan. Tumour load was monitored by bioluminescent imaging twice weekly. Mice were euthanised 21 days post tumour inoculation and *ex vivo* micro-CT was performed on tibiae.

Melphalan treated mice had significantly reduced tumour burden compared to control and losartan only treated mice did not have significantly different tumour burden compared to vehicle control. Using *ex vivo* micro-CT, only the losartan and melphalan group significantly increased trabecular BV/TV% compared to vehicle control (p=0.0190) (Fig1a), and there was a trend for increased trabecular number (p=0.0530) (Fig1b) and cortical thickness (p=0.1552) (Fig1c) in this group compared to control, but it did not reach significance.

In summary, losartan in combination with melphalan showed protection against trabecular bone loss, a trend to protect against cortical bone loss, with no adverse effects on tumour burden. Future work would be to test Losartan in a less aggressive model of myeloma when combined with a standard of care anti-resorptive therapy (zoledronic acid).

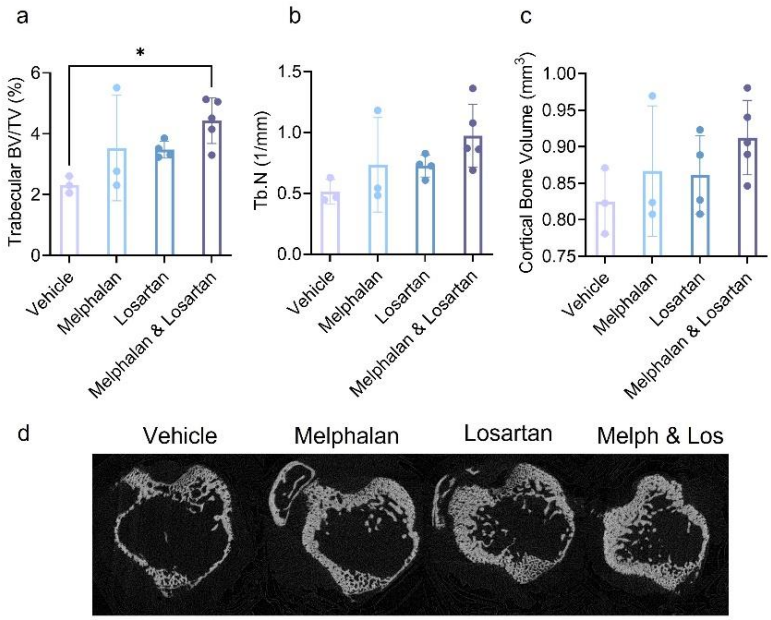

Figure 1: Losartan in combination with melphalan a xenograft model of MM. Ex vivo, left and right tibiae were scanned using Micro-CT. Trabecular and cortical bone analysis was performed using CTan and the average **(a)** trabecular BV/TV, **(b)** trabecular number, and **(c)** cortical bone volume was assessed. **(d)** Representative images slices of Tibiae using CTan.

OC2.3

Mechanical loading of bone suppressed lytic lesion formation and bone loss in a postmenopausal mouse model bearing breast cancer bone metastasis

Norain Ab Latif[1,2], Janet Brown[1], Alison Gartland[1], Ning Wang[1]
[1]The University of Sheffield, Department of Oncology & Metabolism- Medical School, Beech Hill Road- Sheffield S10 2RX, United Kingdom
[2]Universiti Kuala Lumpur Royal College of Medicine Perak, No. 3- Jalan Greentown- 30450 Ipoh, Perak, Malaysia

Abstract Text

Background: Bone metastasis occurs in 70% of advanced breast cancer (BC) patients and reduces the overall survival of these patients to only 2-3 years once diagnosed. Our earlier finding and several other studies have shown that mechanical loading of bone could suppress tumour growth and osteolytic lesion in a BC bone metastasis model in young mice. We now have exciting data on the effect of bone loading in a BC bone metastasis ovariectomised (OVX) mouse model to mimic the postmenopausal BC patients. **Method**: Twenty-two female BALB/c mice (12-week) underwent ovariectomy or sham operation (10-12 mice/group). After a 2-week recovery period, all mice had their right tibia mechanically loaded on 3 alternate days for one week (9N with a 2N pre-load, 40 cycles, 10 second intervals). Mice were then intracardially injected with murine 4T1-Luc2 cells ($5x10^4$ cells/100µl PBS). Tibial loading was continued for another 2 weeks (3x/week) and tumour growth was monitored twice weekly by an in vivo imaging system. Post 3-week of loading, mice were euthanized, tibias were subjected to microCT scanning, bone and lytic lesion analyses and sectioned for tumour burden measurement. The non-loaded left tibias were used as internal controls. **Results**: In tumour-bearing tibias, lytic lesion area was significantly reduced in the loaded tibias of OVX mice (70%, p=0.0227), but not in the sham mice. However, tumour burden did not differ between loaded and non-loaded tibias in either group. In OVX mice, loaded tumour-bearing tibias had higher cortical bone volume (17%, p=0.0359), trabecular bone volume fraction (152%, p=0.0001), thickness (19%, p=0.0103) and number (114%, p=0.0001) with a concomitant decrease in trabecular separation (51%, p=0.0036) compared to the non-loaded counterparts. **Conclusion**: Mechanical loading of bone suppresses osteolysis and bone loss in 'postmenopausal' mice bearing BC bone metastases, thus exercise may serve as an adjuvant treatment for BC patients.

OC3.1

Withdrawn

OC3.2

Impact of menopause and HIV status on the peripheral skeleton of Zimbabwean women

Mícheál Ó Breasail[1], Cynthia Mukwasi-Kahari[2,3], Tafadzwa Madanhire[2,3], Victoria Simms[2,3], Lisa K. Micklesfield[4], Rashida A. Ferrand[2,5], Kate A. Ward[6,7], Celia L. Gregson[8]
[1]University of Bristol, Population Health Sciences, Bristol, United Kingdom
[2]Biomedical Research and Training Institute, The Health Research Unit Zimbabwe THRU ZIM, Harare, Zimbabwe
[3]London School of Hygiene and Tropical Medicine, Department of Infectious Disease Epidemiology, London, United Kingdom
[4]University of the Witwatersrand,
SAMRC/Wits Developmental Pathways for Health Research Unit- Department of Paediatrics- School of Cli nical Medicine, Johannesburg, South Africa
[5]London School of Hygiene and Tropical Medicine, Clinical Research Department, London, United Kingdom
[6]University of Southampton, MRC Lifecourse Epidemiology Centre, Southampton, United Kingdom
[7]London School of Hygiene and Tropical Medicine,
MRC Unit The Gambia at London School of Hygiene and Tropical Medicine, Banjul, Gambia
[8]University of Bristol, Musculoskeletal Research Unit- Bristol Medical School, Bristol, United Kingdom

Abstract Text

Background: Menopause is associated with accelerated bone loss; however, few data are available from sub-Saharan Africa.

Purpose: We aimed to explore whether menopause transition (MT) was associated with bone density and strength in Zimbabwean women living with HIV (WLH) and without (WOH).

Methods: Radius peripheral QCT scans (4% and 33% sites) were obtained from 367 women, aged 40-61 years (n=179[49%] WLH) (Ref: MRCZ/A/2551). Outcomes: Radius 4% total area (Tot.A4, mm^2), total volumetric bone mineral density (Tot.vBMD, mg/cm^3), and compressive bone strength (BSIc, g^2/cm^4); Radius 33% cortical vBMD (Ct.vBMD, mg/cm^3), total area (Tot.A33, mm^2), and Stress-Strain Index (SSI, mm^3). Linear regression was used to produce age, height, and weight adjusted pQCT estimates, mean[95%CI], by menopause stage (pre-, peri-, post-menopause). Tests for trend across menopausal stage are presented. Models were then stratified by HIV status and tested for a HIV*menopause interaction.

Results: Women were of mean(SD) age 50.1(5.8) years and BMI 29.0(6.1) m/kg^2. After adjustment, advancing menopausal stage was associated with lower Tot.vBMD (pre-menopause: 320[310,329] vs. post-menopause: 301[292,311], p-trend=0.026) and BSIc (pre-menopause: 0.36[0.34;0.38] vs. post-menopause: 0.32[0.31,0.34], p-trend=0.023). A similar trend was observed for Ct.vBMD (pre-menopause: 1203[1197,1209] vs. post-menopause: 1176[1170,1182], p-trend<0.001), but not SSI (pre-menopause: 248[241,255] vs. post-menopause: 240[233,248], p-trend=0.20). Total area varied little at either scan site. Stratified by HIV, advancing menopausal stage remained associated with lower Ct.vBMD in both groups, and with lower SSI in WLH only (p-trend=0.019 in WLH, interaction p=0.042).

Conclusion(s): In Zimbabwean women, MT is associated with lower vBMD and strength at the distal radius, a common osteoporotic fracture site. Declines in cortical vBMD were robust to stratification by HIV status, suggesting MT-related cortical deficits are common to both groups. Only WLH had MT-associated declines in predicted bone strength (SSI), potentially indicating earlier cortical bone loss, with implications for fracture risk at other cortical sites (i.e. hip).

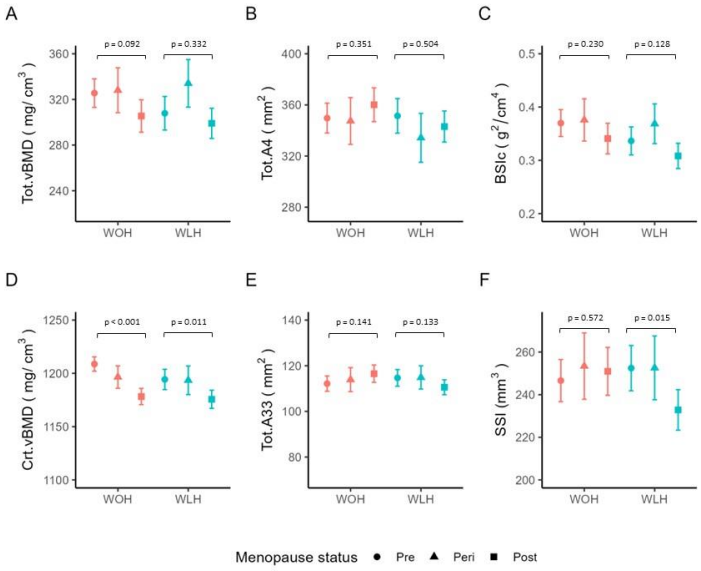

OC3.3

Exposure of osteocytes to diabetogenic glucose reduces differentiation and promotes senescence – a potential explanation for bone fragility in diabetes

Thibault Teissier[1], *Rivka Dressner-Pollak*[2], *Lynne Cox*[1]
[1]*University of Oxford, Department of biochemistry, Oxford, United Kingdom*
[2]*Hadassah Medical Center, Department of Endocrinology and Metabolism, Jerusalem, Israel*

Abstract Text

Introduction: An estimated 415 million people live with diabetes, with serious health consequences that closely mimic 'normal' ageing, suggesting that diabetes causes accelerated ageing. Ageing is associated with accumulation of senescent cells which produce a tissue-remodelling and pro-inflammatory secretome (the SASP). Importantly, older diabetic patients also suffer bone fragility and greatly elevated fracture risk with ageing. We set out to investigate whether this bone fragility may be a consequence of bone cell senescence induced by exposure to glucose concentrations characteristic of diabetes.

Methods: The conditionally immortalised osteoblast cell line IDG-SW3 was differentiated into osteocytes in culture. Cells were exposed to normal glucose concentrations (1g/L) or diabetogenic high glucose concentrations (4.5 g/L) throughout the period of differentiation (compared with mannitol controls for osmotic effects). Cell morphology and proliferation were assessed, together with cell senescence (SA-βgal, p16 and p21 and inflammatory SASP markers). Osteocyte differentiation markers sclerostin, RANKL we measured, and mineral deposition determined by phase contrast microscopy and alizarin red staining.

Results: We find that high glucose concentrations strongly perturb the ability of osteocytes to produce mineral deposits that in vivo would be necessary for maintenance of the inorganic bone matrix. Moreover, high glucose led to reduced sclerostin expression, elevated SA-βgal staining, and cell cycle arrest associated with overexpression of *cdkn2a*(p16) and the receptor for advanced glycation end-products (RAGE), which triggers inflammatory signalling through NFkB. Moreover, *Mtor* expression was greatly increased with high glucose, while mTOR inhibitions rescued some consequences of high glucose, such as p16 expression.

Conclusion: Exposure to diabetogenic glucose impairs osteoblast differentiation into osteocytes and reduces mineral deposition, while increasing cell senescence markers. We suggest that glucose-induced senescence may undermine bone stability in patients with diabetes. We are now exploring whether targeting RAGE and mTOR signalling might alleviate the adverse impacts of high glucose on osteoblasts and osteocytes.

OC4.1

The prevalence and phenotypic range associated with biallelic PKDCC variants

Alistair Pagnamenta[1], *Rebecca Belles*[2], *Bonnie Salbert*[2], *Ingrid Wentzensen*[3], *Maria Sacoto*[3], *Francis Reynoso Santos*[4], *Alesky Caffo*[5], *Matteo Ferla*[1], *Benito Banos-Pinero*[6], *Karolina Pawliczak*[7], *Rosemina Makvand*[8], *Najmabadi Hossein*[9], *Reza Maroofian*[10], *Tracy Lester*[6], *Ana Lucia Yanez Felix*[11], *Camilo Villarroel-Cortes*[11], *Deborah Shears*[12], *Melita Irving*[13], *Amaka Offiah*[14], *Ariana Kariminejad*[8], *Jenny Taylor*[1]

[1]*University of Oxford, Wellcome Centre for Human Genetics, Oxford, United Kingdom*
[2]*Geisinger Health System, Genetics, Danville, United States*
[3]*GeneDx, Clinical Genomics Program, Gaithersburg, United States*
[4]*Children's Hospital of Philadelphia, Division of Human Genetics, Philadelphia, United States*
[5]*Joe DiMaggio Children's Hospital, Clinical Genetics, Hollywood, United States*
[6]*Oxford University Hospitals NHS Foundation Trust, Oxford Genetics Laboratories, Oxford, United Kingdom*
[7]*Guy's Hospital, South East Genomic Laboratory Hub, London, United Kingdom*
[8]*Kariminejad-Najmabadi Pathology & Genetics Center, N/a, Tehran, Iran*
[9]*University of Social Welfare & Rehabilitation Science, Genetics Research Center, Tehran, Iran*
[10]*UCL Queen Square Institute of Neurology, Department of Neuromuscular Diseases, London, United Kingdom*
[11]*National Pediatrics Institute, Human Genetics Department, Mexico City, Mexico*
[12]*Oxford University Hospitals NHS Foundation Trust, Oxford Centre for Genomic Medicine, Oxford, United Kingdom*
[13]*Guy's and St Thomas' NHS Foundation Trust, Department of Clinical Genetics, London, United Kingdom*
[14]*University of Sheffield, Department of Oncology & Metabolism, Sheffield, United Kingdom*

Abstract Text

Background: *PKDCC* encodes a 493 amino-acid component of Hedgehog signalling required for normal chondrogenesis and skeletal development. Although biallelic *PKDCC* variants have been implicated in rhizomelic shortening of limbs with variable dysmorphic features, this association is based on just two patients and limited clinical information has been available.

Purpose: To describe the clinical and genetic features of families with biallelic *PKDCC* variants.

Methods: From a monthly virtual multidisciplinary team meeting that facilitates direct interaction between clinicians and data-analysts, we re-examined unexplained skeletal dysplasia cases from the 100,000 Genomes Project. We used genome sequencing data from the 100,000 Genomes Project in conjunction with exome sequencing results accessed via international collaboration. Sanger sequencing was employed for validation and segregation testing.

Results: We assembled a cohort of 7 individuals from 6 independent families with biallelic *PKDCC* variants and rhizomelic limb-shortening. The allelic series included a previously published splice-donor variant, five frameshifts between codons 77-314 and a missense change observed in two families and supported by *in silico* structural modelling. Two of the frameshifts are in a low complexity GC-rich region and a more systematic analysis of this locus should be considered in clinically suspected cases where a single heterozygous variant is identified. Database queries indicate that the prevalence of

this condition is ~1/424 in clinical cohorts with skeletal dysplasia of unknown etiology. Clinical assessments, combined with data from previously published cases, indicate a predominantly upper limb involvement (Figure). Micrognathia, a prominent forehead, hypertelorism and hearing loss appear to be commonly co-occurring features.

Conclusions: This study confirms the link between biallelic inactivation of *PKDCC* and rhizomelic upper limb-shortening and will enable clinical testing laboratories to better interpret variants in this gene.

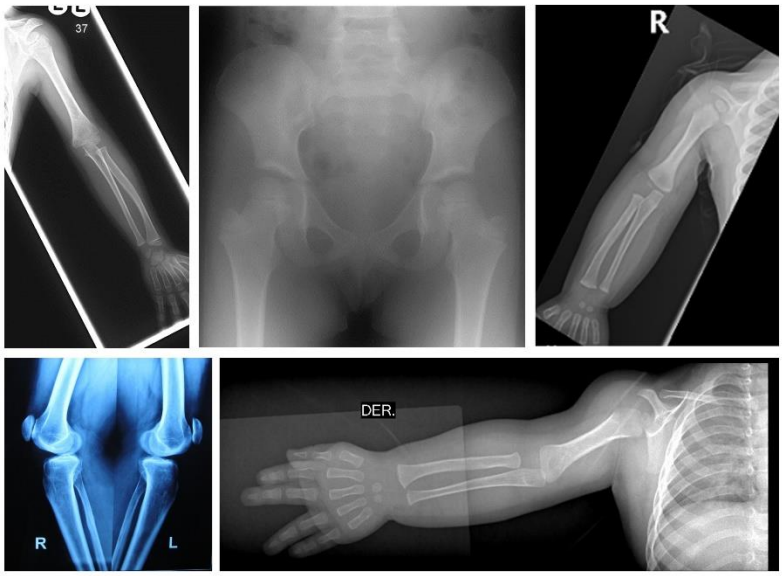

Figure: Radiographic features from families with biallelic inactivation of *PKDCC.*

OC4.2

Injurious hydrostatic pressure induces a reinitiation of developmental processes in murine ex vivo cartilage: an RNAseq study

Lucie Bourne[1], *Aikta Sharma*[2], *Lucinda Evans*[3], *Giselda Bucca*[1], *Andrew Hesketh*[1], *Peter Bush*[1], *Katherine Staines*[1]
[1]*University of Brighton, School of Applied Sciences, Brighton, United Kingdom*
[2]*University College London, Mechanical Engineering, London, United Kingdom*
[3]*Royal Veterinary College, Comparative Biomedical Department, London, United Kingdom*

Abstract Text

Background
Chondrocytes are subject to continuous loads placed upon them throughout development and physical activity. Normal physiological loads enable the maintenance of the articular cartilage health, however abnormal loads contribute to pathological joint ageing. Due to the high-water content of cartilage, hydrostatic pressure is considered one of the main biomechanical influences on chondrocytes and it plays an important role in the mechanoregulation of cartilage.

Purpose
To conduct RNA-seq analysis of hip cap *ex vivo* cultures after physiological and injurious hydrostatic pressure.

MethodsGene expression in *ex vivo* hip cap cultures in response to 5mPa (physiological) or 50mPa (injurious) hydrostatic pressure was quantified by transcriptome analysis using the Illumina platform (n = 4 replicates). For the analysis of differential expression, the transcriptome mapping data for all samples was normalized and analysed using the DESeq2 pipeline. Functional analysis of the groups of differentially expressed genes was performed using clusterProfiler.

Results
Several hundreds of genes were modulated by hydrostatic pressure (375 significantly upregulated and 322 downregulated in 5mPA vs control, and 1022 significantly upregulated and 724 downregulated in 50mPA vs control). Among the genes highly responsive to hydrostatic pressure were Fgf2, Ep300, Ngf, Sox9, Comp, Col6a1 and Col6a2, and Col11a1. Annotations for Biological Processes identified a number of pathways that were upregulated with 50mPa in comparison to control but not in 5mPa including catabolic processes, regulation of developmental growth and regulation of cell size. Biological Processes that were downregulated included chondrocyte differentiation.

ConclusionsInjurious hydrostatic pressure results in a transcriptional induction of genes involved in developmental growth and cell size in *ex vivo* hip cap cultures, suggestive of some of the genetic alterations occurring in osteoarthritis.

OC5.1

Treatment of osteoarthritis by inhibition of aggrecanases using targeted delivery of engineered TIMP-3

Fabio Simoes[1], Ben Alberts[1], Greg Scutt[2], Manuela Mengozzi[1], Katherine Staines[2], Linda Troeberg[3], Andrew Pitsillides[4], Lisa Mullen[1]
[1]Brighton and Sussex Medical School, Department of Clinical and Experimental Medicine, Brighton, United Kingdom
[2]University of Brighton, School of Applied Sciences, Brighton, United Kingdom
[3]University of East Anglia, Norwich Medical School, Norwich, United Kingdom
[4]The Royal Veterinary College, Skeletal Biology Group - Comparative Biomedical Sciences, London, United Kingdom

Abstract Text

Aggrecan loss from articular cartilage driven by the aggrecanases ADAMTS-4 and ADAMTS-5 is a critical early event in osteoarthritis (OA), making these attractive therapeutic targets to slow or prevent the progression of OA. As an endogenous inhibitor of these aggrecanases, tissue inhibitor of metalloproteinase (TIMP)-3 is a promising therapeutic candidate.

To mitigate off-target effects and allow systemic administration of TIMP-3, we leveraged a novel drug-delivery system ("LAP technology"). We have engineered recombinant TIMP-3 linked via a truncated MMP (matrix metalloproteinase) cleavage site with the latency-associated peptide (LAP) from the cytokine TGF-β. We show that TIMP-3 remains latent until release from LAP through MMP activity (Fig. 1a). We also show that there is sufficient MMP activity in human synovial fluid from OA joints to release TIMP-3. Furthermore, cleavage by MMP results in the addition of a leucine residue to the N-terminus of TIMP-3, removing its inhibitory activity for MMPs and thus making it a more targeted therapy towards ADAMTSs. We have demonstrated that upon release from LAP, TIMP-3 retains ADAMTS-4 inhibitory activity.

In ongoing murine studies (approved by the UK Home Office under the UK Animals Scientific Procedures act 1986 and the University of Sussex Animal Welfare and Ethics Review Board), using the destabilisation of the medial meniscus (DMM) model of OA, we are testing the therapeutic efficacy of LAP-MMP-TIMP-3 and a mutant variant (LAP-MMP-mutTIMP-3) designed to increase its bioavailability. Our data show that both variants are able to enter the systemic circulation and reach the diseased joint. Additionally, LAP-MMP-TIMP-3 and LAP-MMP-mutTIMP-3 have preferable pharmacokinetics including significantly reduced clearance rates (Fig 2b; 1.356 mL/min and 1.160 mL/min, respectively; $P < 0.0001$) compared to TIMP-3 on its own (4.568 mL/min). Our data provides encouraging early indications regarding the feasibility of this approach for developing TIMP-3 as a therapeutic for OA.

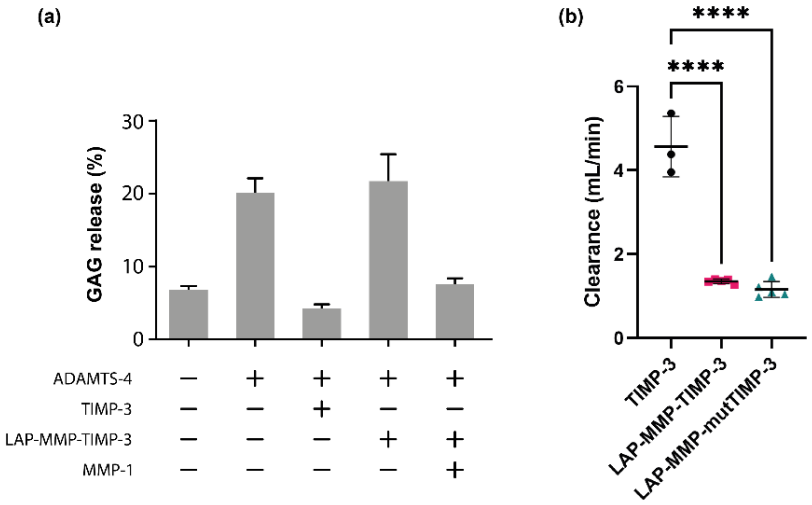

Figure 1. (a) TIMP-3 or LAP-MMP-TIMP-3 was incubated with ADAMTS-4 with or without the presence of MMP-1 prior to addition to bovine cartilage explants. Percentage GAG release was measured by DMMB assay 3 days later. Bars represent mean ± SE of three independent experiments (n = 6). (b) Mice were injected via the tail vein with TIMP-3, LAP-MMP-TIMP-3 or LAP-MMP-mutTIMP-3 and blood samples collected at time points over 4 hours. Levels of the protein were measured via ELISA in the serum collected and a two-compartment model was used to calculate the clearance rate of each protein. One-way ANOVA on Log transformed data showed a significant difference between groups ($P < 0.0001$), with Tukey's post-hoc test showing a significant reduction in clearance rate of LAP-MMP-TIMP-3 ($P < 0.0001$) and LAP-MMP-mutTIMP-3 ($P < 0.0001$) compared to TIMP-3. Bars represent mean ± SD of data from 3 mice for TIMP-3 and 5 mice for LAP-MMP-TIMP-3 and LAP-MMP-mutTIMP-3.

OC5.2

Low operative rates for hip fracture challenge survival in Zimbabwe; findings from the Fractures-E3 Study

Hannah Wilson[1], Anya Burton[1], Ted Manyanga[2], Prudance Mushayavanhu[3], James Masters[4], Simon Graham[4], Munyaradzi Ndekwere[5], Matthew Costa[4], Rashida. A Ferrand[2], Celia. L Gregson[1]
[1]University of Bristol, Musculoskeletal Research Unit, Bristol, United Kingdom
[2]Biomedical Research and Training Institute, The Health Research Unit THRU Zimbabwe, Harare, Zimbabwe
[3]Parirenyatwa Group of Hospitals, Parirenyatwa Group of Hospitals, Harare, Zimbabwe
[4]Nuffield Department of Orthopaedics- Rheumatology and Musculoskeletal Sciences, Oxford Trauma & Emergency Care, Oxford, United Kingdom
[5]Ministry of Health and Child Care, Ministry of Health and Child Care, Harare, Zimbabwe

Abstract Text

Background

As populations age in sub-Saharan Africa, hip fracture rates are predicted to rise, yet data on hip fracture epidemiology are scarce.

Purpose

To characterise the population with hip fractures in Harare, Zimbabwe and understand short-term survival.

Methods

All hip fracture cases presenting to one of seven hospitals in Harare were recorded for one year (10/2021-10/2022), data collected: age, sex, region of residence, presentation date, presentation delays (>2weeks after injury), injury mechanism, fracture type and 30-day survival. Consenting patients completed a researcher-administered questionnaire and anthropometric measurements. Chi-squared tests for associations were used.

Results

We identified 237 hip fracture cases (n=123[51.9%] female), most followed low-energy trauma, e.g. falls (n=207[87.3%]), 81[34.2%] were delayed in hospital presentation. High-energy trauma, e.g. traffic accidents, were more common in men than women (26[22.8%] vs. 4[3.3%], p<0.001), whilst presentation delays were similar (45[36.6%] vs. 36[31.6%] respectively, p=0.42). Overall, 30-day mortality was 10.3%(n=24).

193(81.4%) participants consented to further data collection; mean(SD) age 71.9(14.3)years, 71(43.3%) had a mid-upper arm circumference <25cm (indicating malnutrition), 26(17.2%) were living with HIV (n=25[96%] on treatment). Presentation delays were common (n=68[35.2%]), with 30-day mortality similar in those presenting within 2 weeks of injury (6[8.8%] vs. 12[9.6%], p=0.86). Overall, 113(58.6%)

had an operation; non-operative management was associated with higher 30-day mortality (non-operated 16[20.0%] vs. operated 2[1.8%], p<0.001). Operated and non-operated patients had similar mean[SD] ages (70.7[14.6] vs. 73.2[13.4]years, p=0.23). People attending private vs. public hospitals were more likely to receive an operation (17[85.0%] vs. 96[55.5%], p=0.01).

Conclusion

Hip fractures in Zimbabwe mostly comprise fragility fractures, where malnutrition and HIV infection are common. Non-operative management was common and associated with high mortality, potentially reflecting lack of surgical capacity to offer necessary fixation, avoidance of surgery in multimorbid patients, and/or a patient's inability to pay. Understanding barriers to operative management is important to inform future healthcare delivery.

OC5.3

Withdrawn

OC6.1

Optimisation and characterisation of an adaptable and humanised in vitro 3D self-structuring bone model, capable of long-term osteocyte culture.

Melissa Finlay[1], *Laurence Hill*[2], *Georgiana Neag*[1], *Binal Patel*[1], *Adam McGuinness*[2], *Hannah Lamont*[3], *Kathryn Frost*[1], *Miruna Chipara*[2], *Liam Grover*[4], *Amy Naylor*[5]
[1]*University of Birmingham, Institute of Inflammation and Ageing, Birmingham, United Kingdom*
[2]*University of Birmingham, School of Chemical engineering, Birmingham, United Kingdom*
[3]*University of Bimingham, Institute of Clinical Sciences, Birmingham, United Kingdom*
[4]*University of Birmingham, Healthcare Technologies Institute, Birmingham, United Kingdom*
[5]*University of Birmingham, Institute and Inflammation and Ageing, Birmingham, United Kingdom*

Abstract Text

Background: *In vitro* study of bone metabolism and remodelling has been hampered by an inability to culture osteocytes. The increasing demand for novel therapeutics for bone diseases, and the efforts to replace animals in research, warrants development of such models. Recent advances in 3D *in vitro* cell culture enabled the creation of a self-structuring bone model (SSBM) that supports osteocytogenesis and long-term osteocyte culture, using primary rat periosteal cells (Iordachescu *et al*., 2019). Reported here is the optimisation and characterisation of humanised SSBMs, using a secondary human osteoblast cell line, hFOB 1.19.

Methods and results: hFOB 1.19 cells seeded on a fibrin hydrogel between two calcium phosphate anchors caused gradual matrix contraction and mineralisation (Fig.A). Resultant SSBMs were analysed after 4, 8 and 12 weeks of culture. ELISA, qPCR (Fig.B), and immunofluorescence staining (Fig.C) confirmed differentiation towards osteocytes. Furthermore, XRF and SEM revealed temporal fibrin matrix replacement with a heterogeneously mineralised collagen matrix reminiscent of *in vivo* bone.

Summary: These results demonstrate that SSBM constructs support long-term cell viability, osteocytogenesis (neither of which are achievable in 2D culture (Fig.B)) and osseous matrix development. We are currently investigating the cellular response within SSBM constructs to bone formation modulators and establishing the feasibility of osteoclast co-culture.

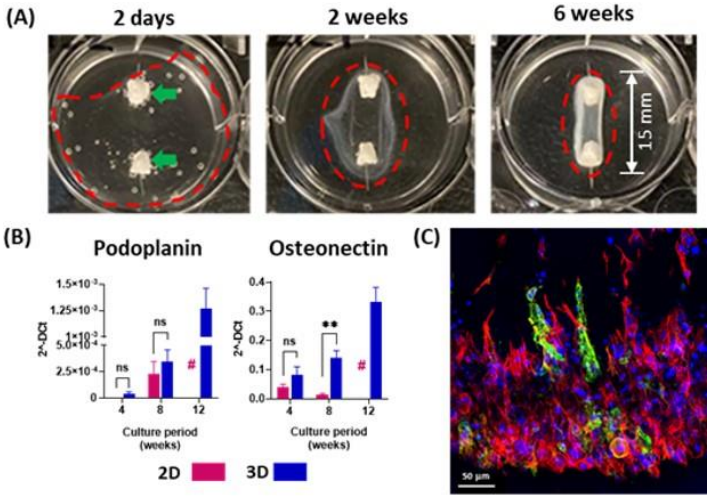

Figure: ***Novel self-structuring bone models (SSBMs) support osteocytogenesis.*** ***(A)*** *Fibrin hydrogel*

*matrix contraction (red line) around the two calcium phosphate anchors (green arrows) post-cell seeding. (**B**) qPCR revealed, at minimum, a 3-fold increased expression of bone cell differentiation and matrix deposition genes over time in 3D (#= 2D culture failure due to extended duration). Data are mean ± SEM. 2D, n=3; 3D, n=4. Statistical analysis by unpaired t-test. ** = P < 0.01; ns = non-significant. (**C**) Immunofluorescence staining after 12-week culture confirmed osteocytic marker expression: Podoplanin (green), Actin (Phalloidin-488, red), Nuclei (Hoechst, blue). Scale bar = 50µm*

OC6.2

Condylar asymmetry in the knees of osteoarthritic mice

Lucinda Evans[1], *Andrew Bodey*[2], *Peter Lee*[3], *Andrew Pitsillides*[1]
[1]*Royal Veterinary College, Comparative Biomedical Sciences, London, United Kingdom*
[2]*Diamond Light Source, Harwell Campus, Didcot, United Kingdom*
[3]*University College London, Mechanical Engineering, London, United Kingdom*

Abstract Text

Background - Predisposition to osteoarthritis (OA) in humans is linked to gross anatomical features with biomechanical consequences. STR/Ort mice develop age-related OA, spontaneously in the medial tibia, whilst parental CBA controls age healthily, yet differences in their condylar anatomy remain uncharacterised.

Purpose**:** To describe tibial and femoral epiphyseal anatomy in STR/Ort and CBA mice, enabling estimation of its contribution to OA.

Methods: Knee joints from male STR/Ort and CBA mice, killed at ~10, ~20, or 36+ weeks (total n = 24), were fresh-frozen until high-resolution (pixel=1.625µm) synchrotron scanning at -20°C (Diamond Light Source, session MG28353). The investigator was blinded, reconstructed scans were oriented in Dataviewer, and femoral and tibial condylar width and angle were manually measured in Fiji; the former was used to quantify latero-medial symmetry. Data were statistically analysed in SPSS by Kruskal-Wallis with Bonferroni correction. All procedures aligned with the Animals (Scientific Procedures) Act 1986 and study design was approved by local Ethical Review.

Results: CBA showed more symmetrical condylar anatomy than STR/Ort mice (p=0.020), particularly in the femur, with only 59% of CBA possessing wider medial than lateral condyles, versus 100% of STR/Ort mice. Tibial symmetry was influenced by age, increasing significantly in both strains from 10-20 weeks (p = 0.025). Lateral and medial femoral condyles exhibited no significant width or angle difference. However, medial tibial condyle surface (median=10.1^{o}) was significantly more angled than the lateral condyle (median=4.1^{o}, p = 0.001). Lateral tibial condyles (median=1037µm) were significantly wider than medial tibial condyles (median= 851µm, p = 0.018).

Conclusions: Relatively asymmetrical condyles in STR/Ort mice aligns with prior research that disclosed greater walking gait asymmetry than in CBA mice, which also corresponded with OA severity. Future research may clarify whether condylar asymmetry is a cause or effect of asymmetric weight-bearing, and whether it also serves to predict OA severity.

OC6.3

Permeabilisation of Cells Using Ultrasound Stimulated Microbubbles for Bone Fracture Repair

Oliver Pattinson[1], Sam Sloan[1], Mohamed Mousa[2], Nicholas Evans[1], Dario Carugo[3], Fabrice Pierron[2], Janos Kanczler[2], Simon Tilley[4]
[1]University of Southampton, Faculty of Engineering and Physical Sciences, Southampton, United Kingdom
[2]University of Southampton, Faculty of Medicine, southampton, United Kingdom
[3]University College London, School of Pharmacy, London, United Kingdom
[4]University Hospital Southampton, Orthopaedics, Southampton, United Kingdom

Abstract Text

Introduction: Non-union or delayed-union fracture is a debilitating condition with a high healthcare burden. Present therapies are invasive, possibly ineffective, and have associated risks of infection. Remote targeting of bone fracture sites using circulating ultrasound-responsive microbubbles offers a promising method for noninvasive targeted drug delivery[1]. These therapies rely on cavitation mechanics to induce reversible permeabilisation of cells to allow a transfer of molecules across the membrane. In this study, we hypothesized that ultrasound stimulation of bone marrow stromal cells (BMSCs) in the presence of microbubbles would enhance cell permeability.

Methods: Microbubbles were made by thin film hydration of DSPC and PEG40 stearate at a 9:1 molar ratio, followed by hydration in PBS and sonication at the air/liquid interface. BMSC isolated from human volunteers were cultured in 35mm diameter ibidi dishes in the presence and absence of microbubbles. Using a compact acoustic device[2]. Cultures were acoustically stimulated at varying peek negative pressure from 0-0.5MPa and duty cycle 10-50% in the presence of the cells. Propidium iodide (PI) added before sonication was used as a fluorescent marker to indicate permeabilization of a cell and fluorescence microscopy and image analysis was used to measure permeability.

Results: A significant increase in the number of permeable BMSCs was observed for acoustic pressures greater than 0.2MPa. An average of 15.0 ±9.8, 13.3 ±7.6 and 14.6 ± 6.6 cells showing PI uptake were observed under acoustic pressures of 0.3MPa, 0.4MPa and 0.5MPa respectively ($p < 0.001$) compared to 0.5 ± 0.9 and no permeable cells in both an ultrasound alone and microbubble alone control test respectively. Changing the duty cycle of the pulse regime was shown to have no significant effect on the number of permeable cells.

Conclusions: To conclude, successful application of microbubble stimulation for bone cell permeabilization is demonstrated for pressures in vitro, demonstrating the potential for localised, bone repair-specific drug delivery.

BRS Poster Pitching Abstracts

P006

Longitudinal size-adjusted bone density outcomes in peripubertal children living with HIV

Lisha Jeena[1], Anthony Hsieh[1], Ruramayi Rukuni[2,3], Vicky Simms[2,4], Cynthia Mukwasi-Kahari[2,4,5], Grace McHugh[2], Joseph Chipanga[6], Suzanne Filteau[4], Hilda Mujuru[7], Sarah Rowland-Jones[1], Celia L Gregson[2,8], Rashida A Ferrand[2,3]
[1]University of Oxford, Nuffield Department of Medicine, Oxford, United Kingdom
[2]Biomedical Research and Training Institute, The Health Research Unit THRU Zimbabwe, Harare, Zimbabwe
[3]London School of Hygiene and Tropical Medicine, Clinical Research Department, London, United Kingdom
[4]London School of Hygiene and Tropical Medicine, Department of Infectious Disease Epidemiology, London, United Kingdom
[5]Bristol Medical School, Population Health Sciences, Bristol, United Kingdom
[6]Biomedical Research and Training Institute, The Health Research Unit THRU, Harare, Zimbabwe
[7]University of Zimbabwe, Department of Paediatrics, Harare, Zimbabwe
[8]Bristol Medical School- University of Bristol, Musculoskeletal Research Unit, Bristol, United Kingdom

Abstract Text

Background/purpose:

During puberty substantial bone mass is accrued. We sought to investigate how bone mass changes over a one-year period in peripubertal children living with HIV (CWH) compared to children without HIV (CWOH) in Zimbabwe.

Methods:

CWH, on ART for ≥2 years, and CWOH, aged 8-16, were recruited from clinics and schools. DXA scans at baseline and 12-month follow-up measured height-adjusted total body less-head bone mineral content (TBLH-BMC) and lumbar spine bone mineral apparent density (LS-BMAD) Z-scores, with annualised change calculated. Best fit plots visualised the association between age and change in bone outcomes. Sex-stratified linear regression compared bone outcomes by HIV status, adjusting for age, pubertal stage and baseline Z-score.

Results:

There were 244 CWH (mean age 13.0 years (SD 2.3), 119 (48.8%) girls) and 248 CWOH (mean age 12.9 years (SD 2.4), 126 (50.8%) girls). Fewer CWH had reached Tanner stage V compared to CWOH (7.0% vs 14.1%). CWH had lower mean Z-scores for LSBMAD (-0.72 (SD 1.40) vs -0.28 (SD 1.21)) and TBLH-BMC (-0.79 (SD 1.10) vs -0.46 (1.03)) compared to CWOH. Before adjustment, HIV was associated with less gain in bone mass compared to CWOH, particularly among boys (Figure 1). After one year, bone gains were similar in girls with and without HIV: adjusted mean difference in LS-BMAD Z-score 0.05 [95%CI: -0.12,

0.12]; p=0.93, and TBLH-BMC Z-score 0.11 [-0.02, 0.25]; p=0.11. However, boys living with HIV gained less TBLH-BMC Z-score (0.15 [95%CI: -0.09, -0.31]; p<0.001) compared to boys without HIV, whilst changes in LS-BMAD Z-score were similar (0.06 [-0.44, 0.55]; p=0.850).

Conclusion:

Boys with HIV have evidence of impaired bone accrual, independent of delayed pubertal development, with implications for future peak bone mass and adult fracture risk. This research contributes to the limited literature which investigates longitudinal bone accrual in CWH. Longer term follow-up studies are needed.

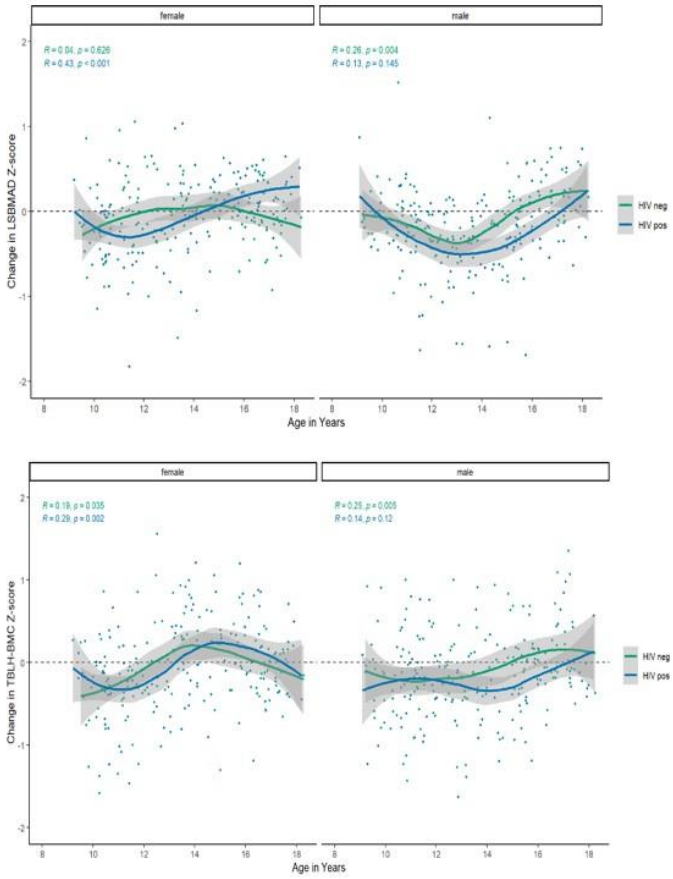

Figure 1: (a) Change in LSBMAD and (b) TBLH-BMC Z-scores by HIV status between 8 and 18 years old

P007

Establishment and characterisation of doxorubicin resistant osteosarcoma cell line variants with increasing resistance

Victoria Tippett[1], *Luke Tattersall*[1], *Michelle Lawson*[1], *Alison Gartland*[1]
[1]*University of Sheffield, Oncology and Metabolism, Sheffield, United Kingdom*

Abstract Text

Introduction: Osteosarcoma is a rare often fatal type of primary bone cancer that is treated with methotrexate, doxorubicin and cisplatin. Unfortunately, up to 68% of patients respond poorly with no change in treatment options and survival statistics in over 40 years. There is therefore an urgent need to understand chemoresistance in order to improve survival.

Methods: We have developed three variants with increasing doxorubicin resistance from the metastatic osteosarcoma cell line 143b-GFP+LUC. Our models were characterised *in vitro* by assessing metabolic growth rate, migration and mineralisation in order to determine how resistance affects these outcomes.

Results: We have established doxorubicin resistance in variant 1 (10.29-fold), 2 (9.066-fold) and 3 (64.98-fold) compared to the 143b-GFP+LUC control cell line. There was a significant increase in resistance in variant 3 compared to the control and earlier variants ($P<0.0001$, Tukey's test). Between variants 1 and 2 there was no difference in resistance.

The growth of the control cell line was significantly greater than all variants on day three ($P<0.0001$, Tukey's test). Variant 3 grew significantly slower than variant 1 ($P=0.0149$) and 2 ($P=0.0023$). The estimated growth rate was 11.8hr for the control cell line, 13.6hr for variant 2, 13.9hr for variant 1 and 16.4hr for variant 3.

All three variants had a significantly larger migration wound area at 39.4%, 40% and 42.4%, respectively, in comparison to the control cell line which had all but closed by 16hrs ($P<0.0001$, Tukey's test). There was no difference in migration between variants ($P>0.9458$) suggesting migration is unaffected by increasing resistance.

Interestingly when we assessed mineralisation under increasing concentrations of doxorubicin, the phenotypic pattern of mineralisation noticeably differed across variants compared to the control cell line.

Conclusion: We have determined that doxorubicin resistance in osteosarcoma reduces cell growth and migration and alters the pattern of mineralisation under DOX pressure.

P008

The Additive effect of Vitamin K Supplementation and Bisphosphonate on Fracture Risk in Post-menopausal Osteoporosis : a randomised placebo controlled trial

Amelia Moore[1], Dwight Dulnoan[2], kieran Voong[3], Salma Ayis[4], Anastasios Mangelis[4], Renata Gorska[5], Dominic Harrington[5], William fraser[6], Geeta Hampson[7]
[1]Kings College london, Osteoporosis Unit- Guy's Hospital, London, United Kingdom
[2]Guys and St Thomas NHS Trust, Osteoporosis Unit- Guy's Hospital, London, United Kingdom
[3]Synnovis Analytics, Nutristasis Unit- St Thomas' Hospital, London, United Kingdom
[4]Kings College London, School of life Course and Population Sciences- Guy's Campus, London, United Kingdom
[5]Synnovis Analytics, Nutristasis Unit- St Thomas Hospital, London, United Kingdom
[6]University of East Anglia, Norwich Medical School-, Norwich, United Kingdom
[7]Guys and St Thomas Hospital/Kings College London,
Department of Chemical Pathology/Metabolic Medicine, London, United Kingdom

Abstract Text

Background. Vitamin K acts as a co-factor in the carboxylation of vitamin K dependent proteins (VKDPs) which includes proteins present in bone such as osteocalcin (OC). This process confers biological activity to the VKDPs and in the case of OC, increases its affinity for bone hydroxyapatite. Clinical studies have suggested that vitamin K prevents bone loss and may improve fracture risk.

Purpose. The aim of this study was to assess whether vitamin K supplementation has an additive effect on bone mineral density (BMD), hip geometry and bone turnover markers (BTMs) in post-menopausal women with osteoporosis (PMO) and sub-optimum vitamin K status.

Methods. We conducted a randomized placebo-controlled trial in 105 postmenopausal women aged 68.7[12.3] years with PMO and serum vitamin K1 ≤0.4 µg/L. Following informed consent, they received vitamin K_1 (1 mg/day) or vitamin K_2 (MK4 45 mg/day) or placebo for 18 months. All 3 groups were on oral bisphosphonate and calcium and/or vitamin D. We measured BMD by DXA, derived hip geometry parameters using hip structural analysis (HSA) software and BTMs. Intention to treat (ITT) and per protocol (PP) analyses were performed.

Results. BMD at the total hip (TH), femoral neck (FN) and lumbar spine (LS) and changes in the BTMs; CTX and P1NP did not differ significantly between the 3 groups. Following PP analysis and correction for covariates, there were significant differences in some of the HSA parameters at the intertrochanter (IT) and femoral shaft (FS) : IT endocortical diameter (ED) (% change placebo: 1.5 [4.1], K_1 arm: -1.02 [5.07], *p=0.04*), FS subperiosteal/outer diameter (OD) (placebo : 1.78 [5.3], K_1 arm: 0.46 [2.23] *p=0.04*), FS cross sectional area (CSA) (placebo:1.47 [4.09],K_1 arm: -1.02 [5.07], *p=0.03*).

Conclusion. The addition of vitamin K_1 to oral bisphosphonate in PMO may have an effect on parameters of hip geometry. Further confirmatory studies are needed.

P009

Mapping 3D variation in epiphyseal architecture reveals distinct spatially-conserved patterns of bone organisation in normal canine femoral heads: a foundation for early OA detection

Gareth Jones[1], *Andrew Pitsillides*[2], *Richard Meeson*[1]
[1]*Royal Veterinary College, Clinical Science and Services, London, United Kingdom*
[2]*Royal Veterinary College, Comparative Biomedical Sciences, London, United Kingdom*

Abstract Text

Background:
Debilitating and painful hip osteoarthritis (OA) is common in dogs and humans, yet its early radiographic detection remains enigmatic. Here, we use non-destructive imaging to 3D map bone architecture utilising a *whole* bone approach, to define conserved spatial patterns of epiphyseal architecture within non-diseased canine femoral heads; this will substantiate a foundation against which early OA detection is rendered viable.

Methods:
Non-diseased canine femoral heads (n=28) were imaged ex-vivo using micro-computed tomography and analysed utilising a novel whole bone approach. This involved 3D segmentation of the entire epiphysis, divided into two concentric rings (inner/outer), subdivided into quadrants creating eight anatomically-mapped segments (Figure A). Cortical and trabecular bone were separated, and 3D morphometric analyses performed. Ethical approval was granted for use of residual clinical samples.

Results:
Analysis identified statistically significant 3D variation with trabecular percentage bone volume ($p<0.001$), trabecular spacing ($p=0.002$), degree of anisotropy ($p<0.001$) and cortical thickness ($p<0.001$). Intriguingly, further interrogation identified *two* distinct prevailing spatially-conserved patterns. Firstly, a *quadrant* pattern – both inner and outer segments within each quadrant mirroring each other with the variation existing between the quadrants – for trabecular percentage bone volume and cortical thickness (Figure B) where the patterns appeared to mirror the load-bearing function of these quadrants. Secondly, a *concentric* pattern, where variation was between inner and outer rings, for trabecular spacing, trabecular number and degree of anisotropy (Figure C), where the inner ring closer to the centre contained more numerous, closer together trabeculae with a greater degree of spatial disorganisation than the outer peripheral ring.

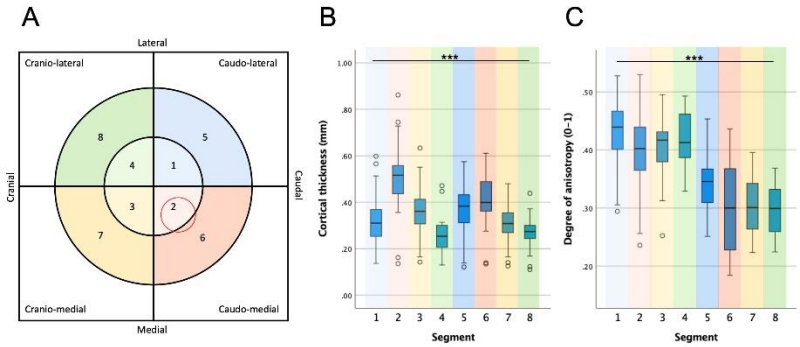

Figure A-C: (A) 2D Schematic representation of the novel segmentation methodology. Box and Whisker plots for Cortical Thickness (B) and Degree of Anisotropy (C). *** Indicated $p<0.001$

Conclusion:

Accurate 3D mapping of epiphyseal architecture reveals highly conserved spatial relationships within the cortical and trabecular compartments. Precise defining of this spatial variation in epiphyseal architecture of normal femoral heads provides a foundation for more accurate mapping of spatial relationship between cartilage degeneration and subchondral remodelling in OA.

P010

Myeloma cell dormancy on 3D in vitro PolyHIPE scaffold models

Alexandria Sprules[1], *Mina Aleemardani*[2], *Caitlin Jackson*[2], *Georgia Stewart*[1], *Alanna Green*[1], *Frederik Claeyssens*[2], *Michelle Lawson*[1]
[1]*The University of Sheffield, Oncology and Metabolism, Sheffield, United Kingdom*
[2]*The University of Sheffield, Department of Materials Science and Engineering, Sheffield, United Kingdom*

Abstract Text

Relapse remains an obstacle for patients with multiple myeloma (MM), despite continued improvements in treatments. Dormant myeloma cells (DMCs) have been observed in 2D *in vitro* cultures and *in vivo,* where they reside in endosteal niches and interact with osteoblasts to maintain their dormancy. Importantly, DMCs may be implicated in MM relapse, thus represent an important target. However, *in vitro* models often fail to replicate the complex *in vivo* bone marrow microenvironment (BMM). Furthermore, with an ever-shifting motivation to uphold the principles of the 3Rs (to reduce, replace and refine *in vivo* studies), alternative 3D models using synthetic materials are a favourable candidate to achieve partial replacement of resource-intensive, technically demanding animal models. The use of 3D *in vitro* models may recapitulate the *in vivo* BMM in an *in vitro* setting, therefore the objective of this study was to assess the suitability of 3D polycaprolactone-based polymerised high internal phase emulsion (PolyHIPE) scaffolds for the generation of DMCs.
PolyHIPE scaffolds were pre-seeded with osteoblast cells prior to the addition GFP tagged, 1,1'-dioctadecyl-3,3,3',3'-tetramethylindodicarbocyanine (DiD) stained myeloma cells (MCs). Over 21 days, MCs were assessed via fluorescent microscopy and flow cytometry for DiD retention and cell viability was assessed via an alamarBlue™ assay.
The PolyHIPE model facilitated growth of MCs without toxicity, ingrowth and clustering of MCs was observed throughout the scaffold. DMCs (defined as DiD-high) were present on the PolyHIPE scaffolds (DMCs represented 0.038% of all MCs at day 21) but did not penetrate the scaffold, remaining on the scaffold surface. Furthermore, cell growth is potentially altered upon changing the parameters of the PolyHIPE scaffold.
In summary, cell biocompatibility and the presence of DMCs on the PolyHIPE scaffolds was demonstrated. Further refinement of the scaffold properties should facilitate generation of DMCs in additional cell lines and patient samples for future drug testing.

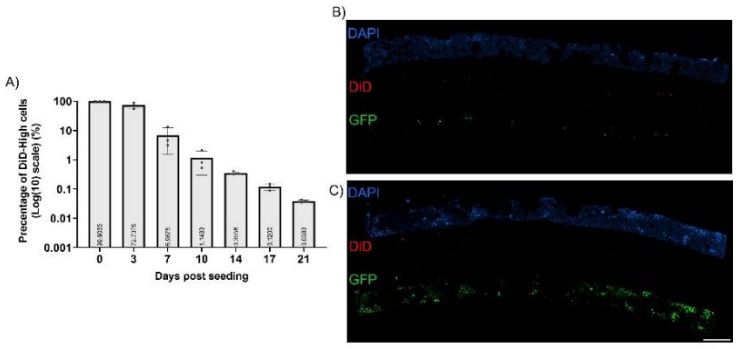

Figure 1. DiD retention of 5TGM1 cells within PolyHIPE scaffolds. GFP tagged 5TGM1 cells were stained with DiD (day 0) and cultured on PolyHIPE scaffolds pre-seeded with MC3T3 cells for 21 days. A) At regular intervals, 5TGM1 cells were isolated from the scaffold and the percentage of dormant 5TGM1 cells (GFP+ DiD-high) present on the scaffold was examined via flow cytometry (n=3). Visualisation of dual labelled 5TGM1 cells within a cross section of the PolyHIPE scaffold at B) day 7 and C) day 21 confirmed retention of DiD in a small population of cells and the ingrowth of DiD-negative GFP+ proliferating cells throughout the scaffold. Autofluorescence of the PolyHIPE scaffold is observed via the DAPI channel, 5TGM1 cells identified via the GFP channel and DMCs identified by overlap of GFP and DiD channels. Scale bar = 350 μm.

P015

Withdrawn

P051

Extent of Abdominal Aortic Calcification is Associated with Increased Risk of Rapid Weight Loss over 5 years: the Perth Longitudinal Study of Ageing Women

Cassandra Smith[1], Marc Sim[2], Jack Dalla Via[2], Abadi K. Gebre[2], Kun Zhu[3], Wai H. Lim[3], Douglas P. Kiel[4], John T. Schousboe[5], Itamar Levinger[6], Stephan von Haehling[7], Andrew J. S. Coats[8], Richard L. Prince[3], Joshua R. Lewis[2]
[1]Edith Cowan University, Nutrition & Health Innovation Research Institute, Perth, Australia
[2]Nutrition & Health Innovation Research Institute- School of Medical and Health Sciences, Edith Cowan University, Perth, Australia
[3]Medical School, The University of Western Australia, Perth, Australia
[4]Marcus Institute for Aging Research- Hebrew SeniorLife- Department of Medicine Beth Israel Deaconess Medical Center, Harvard Medical School- Boston, Boston, United States
[5]Division of Health Policy and Management, University of Minnesota, Minneapolis, United States
[6]Institute for Health and Sport IHES, Victoria University, Melbourne, Australia
[7]Department of Cardiology and Pneumology, University of Goettingen Medical Center, Goettingen, Germany
[8]Heart Research Institute, Sydney, Sydney, Australia

Abstract Text

Introduction: Abdominal aortic calcification (AAC), a marker of vascular disease, is associated with increased falls and fracture risk in older adults.

Purpose: We hypothesized that AAC is related to rapid weight loss, a risk factor for musculoskeletal disease, over 5 years in community-dwelling older women (n = 929, mean±SD age = 75.0 ± 2.6 years).

Methods: Lateral spine images from DXA (1998/1999) were used to assess AAC using the 24-point scoring method (AAC-24). Over 5 years, body weight was assessed at 12-month intervals. Rapid weight loss, defined as >5% decrease in body weight in any 12-month period. Multivariable adjusted logistic regression was used to assess the relationship between AAC and rapid weight loss.

Results: During follow-up, 366 women experienced rapid weight loss. For each point increase in AAC-24, women had 6% greater odds of having rapid weight loss (odds ratio [OR] 1.06 CI 1.02-1.10). Compared to women with low AAC (0-1), those with moderate (2-5) and extensive AAC (≥6) had higher odds for presenting with rapid weight loss (OR 1.37 CI 1.01-1.86, OR 1.60 CI 1.10-2.32, respectively). The model estimates were similar after adjusting for alcohol, protein, total fat and carbohydrate intake, overall diet quality, grip strength, and timed up-and-go. In subgroups of women who met protein intake/physical activity recommendations the associations were similar (extensive vs low AAC: OR 1.78 CI 1.11-2.87, OR 1.57 CI 1.02-2.43).

Conclusions: AAC extent was associated with greater risk for rapid weight loss over 5 years in older women. Since the association was significant even after taking nutritional intakes into account, these data support the possibility that vascular disease plays a role in the maintenance of body weight. Whether AAC is a marker of vascular disease of other vascular beds essential for nutrient absorption and losses of lean mass and explains the weight loss association should be explored.

P076

Determining the Origin and Function of Matrix Bound and Secreted Vesicles in Mineralisation

Evie Anghileri[1], *Ignacio Martin-Fabiani*[2], *Owen Davies*[1]
[1]*Loughborough University, School of Sport- Exercise and Health sciences, Loughborough, United Kingdom*
[2]*Loughborough University, Materials, Loughborough, United Kingdom*

Abstract Text

Background: Effective therapies for skeletal regeneration are of increased importance with bone representing the second most transplanted tissue worldwide. With available therapies presenting limitations, the delivery of natural extracellular vesicles (EVs) as an acellular biological therapy presents a novel alternative. However, EVs are highly heterogenous, with distinct fractions of secreted (sEV) and matrix-bound vesicles (MBV) implicated in skeletal development.

Purpose: The present study aimed to compare the origin and relative pro-mineralising properties of MBVs and sEVs to define an optimal population for future regenerative therapies.

Methods: sEVs and MBVs were isolated from murine MC3T3 and mineralising primary human MSC cultures on day 2, 7, 14 and 21 of mineralisation. sEVs were isolated from EV-depleted culture medium by ultracentrifugation. MBVs were isolated from the matrix using collagenase digestion. Markers of endosomal-origin biogenesis and pro-mineralising potential were compared using ALP assays, Western blots, nano-flow cytometry and super resolution microscopy. Immunoprecipitation was applied to further enrich the MBV fraction for Annexin proteins implicated in calcium influx.

Results: Western blots demonstrated an upregulation of endosomal-origin biogenesis markers CD9 and CD63 alongside putative pro-mineralisation markers ALP, Annexin V and Annexin II in MBV comparable to sEV fractions across mineralisation. ALP expression increased over the 21-day mineralisation period in sEV fractions ($p<0.05$). ALP protein content increased until day 7 in MBV fractions ($p<0.05$) followed by a subsequent decrease. At each time point analysed, ALP was markedly higher in MBV compared to sEV fractions ($p<0.05$) (Figure 1). MBV fractions enriched in Annexin V demonstrated presence of other pro-mineralisation markers suggesting a potential cooperative relationship.

Conclusions: These data suggest that MBVs may represent a subset of secreted endosomal vesicles (e.g. 'exosomes') that become anchored into the matrix, which have a markedly enhanced mineralisation capacity. Further work will assess the functional capacity of each population in vitro.

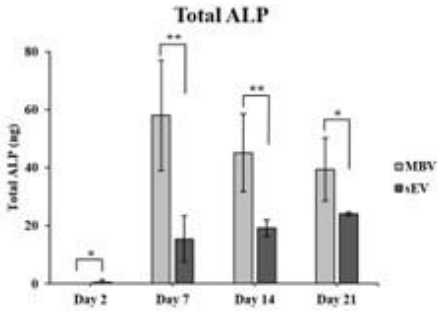

P084

Altered biomechanics in prostate cancer patients following ADT

Fiona Gibson[1], *Margaret Paggiosi*[2], *Catherine Handforth*[2], *Janet Brown*[2], *Enrico Dall'Ara*[2], *Stefaan Verbruggen*[1]
[1]*The University of Sheffield, Department of Mechanical Engineering, Sheffield, United Kingdom*
[2]*The University of Sheffield, Department of Oncology and Metabolism, Sheffield, United Kingdom*

Abstract Text

Background

Androgen deprivation therapy (ADT) is the standard of care for advanced prostate cancer (PC). However, ADT is associated with a decrease in areal bone mineral density (aBMD) [1] and an increase in fracture risk [2]. Areal BMD, measured by DXA, only accounts for 40% of overall fracture risk [3] and it is important to also consider bone quality. DXA is not able to assess bone quality as it depends on multiple factors including bone microarchitecture and strength [3]. Therefore, to fully capture fracture risk, a quantitative evaluation of the whole bone biomechanics is necessary.

Purpose

To assess the effects of 12 months of ADT on vertebral mechanical properties in patients with PC.

Methods

Dataset included PC patients receiving ADT (n=20). 3D finite element (FE) models of the T12 vertebra were reconstructed from QCT scans performed at baseline and 12 months. Bone was modelled as heterogenous, isotropic, and elastic-plastic, with material properties based on patient-specific densitometry calibration and phenomenological relationships. FE analysis simulated failure by compression (1.9% strain) to analyse the structural and mechanical properties.

Results

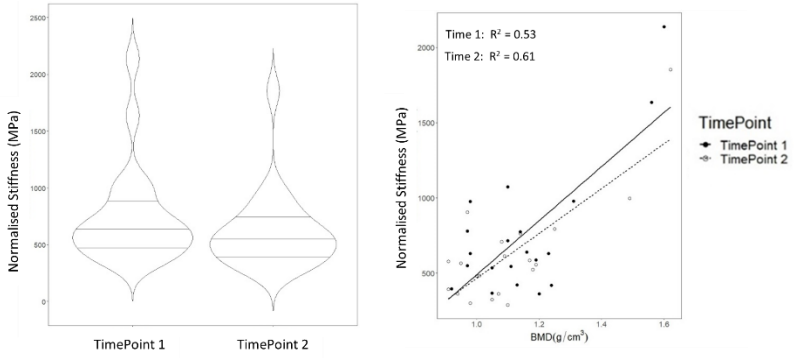

Figure1.(A)Violin plot of the normalised stiffness at two timepoints with the median and interquartile ranges. (B)Linear regression between normalised stiffness and vBMD for both timepoints.

Stiffness decreased significantly (p=0.006) between baseline (758±444 MPa) and 12 months (622±351 MPa). The average volumetric BMD (vBMD) also decreased (baseline=1.15±0.18 g/cm^3, 12 months=1.10±0.18 g/cm^3, p=0.0002).

Conclusion

The goodness-of-fit for the models between vBMD and stiffness (R^2=0.53 and R^2=0.61) demonstrates that vBMD alone cannot predict the biomechanical properties for individual patients. Although higher vBMD values do correlate with higher stiffness, bone architecture and more mineralized cortical tissue have a notable effect on vertebral mechanical properties. This suggests that the in-clinic assessment alone is not sufficient to define fracture risk and further biomechanical investigations are necessary.

[1]Abrahamsen et al.,*BJU Int.*,2007

[2]Shahinian et al.,*J Med. Branch*,2022

[3]Bienz et al.,*Bonekey Rep.*,2015

P181

P53 regulates mitochondrial dynamics in vascular smooth muscle cell calcification.

Kanchan Phadwal[1], Mathew Horrocks[2], Ineke Luijten[3], Jin Feng Zhao[4], Qiyu Tang[1], Robert Semple[3], Ian Ganley[4], Vicky MacRae[1]
[1]The Roslin Institute & RDSVS- University of Edinburgh- Easter Bush- Midlothian- EH25 9RG- UK, Functional Genetics, Midlothian, United Kingdom
[2]School of Chemistry- Joseph Black Building- David Brewster Road- University of Edinburgh- EH9 3FJ, Chemistry, Edinburgh, United Kingdom
[3]Queens Medical Research Institute- Edinburgh Bioquarter- 47 Little France Crescent- Edinburgh- EH16 4 TJ- UK, Cardiovascular science, Edinburgh, United Kingdom
[4]University of Dundee- Sir James Black Centre'- Dundee- DD1 5EH- UK, MRC Protein Phosphorylation & Ubiquitylation Unit, Dundee, United Kingdom

Abstract Text

Introduction: Arterial calcification is an important characteristic of cardiovascular disease. Calcifying vascular smooth muscle cells (VSMCs) show reduced oxygen consumption rate and ATP linked respiration, suggestive of dysregulated mitochondrial activity. However, molecular mechanisms linking mitochondrial dysfunction and arterial calcification have yet to be determined

Purpose: To examine mitochondrial dynamics in VSMC calcification.

Methods: VSMCs isolated from the aorta of 5-week-old C57BL6 mice were calcified in 3mM phosphate (Pi) for 14 days for immunofluorescence and immunoblotting studies. Aorta from mito-QC mice (express a mitochondrial outer membrane-targeted tandem mCherry-GFP-tag) were used for imaging mitochondrial dynamics. Mitochondrial fractions were isolated using commercial kits.

Results: Pi-induced VSMC calcification was associated with elongated mitochondria (3.04-fold increase, *p<0.001*), increased mitochondrial ROS production (2 fold increase; *p<0.001*) and reduced mitophagy (14.5-fold decrease; p<0.01). An increase in protein expression of Optic Atrophy Protein 1 (OPA1; 2.0-fold increase, *p<0.05*) and a converse decrease in expression of Dynamin-related protein 1 (Drp1*;* 1.6-fold decrease *p<0.05*), two crucial proteins required for the mitochondrial fusion and fission process respectively, were noted too. Furthermore, the phosphorylation of Drp1 Ser637 was increased in mitochondria from calcified VSMCs (2.8-fold increase; P<0.05), suppressing mitochondrial translocation of Drp1. Calcified VSMCs show enhanced p53 expression (6.1-fold increase, p<0.05) and β-galactosidase activity (1.8-fold increase, p<0.001), both associated with cellular senescence. siRNA-mediated p53 knockdown reduced calcium deposition (4-fold decrease; P<0.01), mitochondrial length (3.0 fold decrease, P<0.001) and β-galactosidase activity (2.4-fold decrease, P<0.001), with concomitant mitophagy induction (3 fold increase, P<0.05). Reduced OPA1 (2.9-fold decrease, *p<0.05*) and increased DRP1 protein expression (2.6 fold increase*; p<0.05*) with decreased phosphorylation of Drp1 Ser637 (6.83-fold decrease, p<0.05) was also observed upon p53 knockdown in calcifying VSMCs.

Conclusions: p53 modulates DRP1 to regulate mitochondrial morphology and function in arterial calcification. Targeting mitochondrial dynamics may represent a new focus for clinical treatment.

P185

A new toolkit for studying matrix vesicles using biorthogonal click chemistry and correlative light-electron microscopy

Scott Dillon[1], *Melinda Duer*[1]
[1]*University of Cambridge, Yusuf Hamied Department of Chemistry, Cambridge, United Kingdom*

Abstract Text

Background: Matrix vesicles (MVs) are ~150nm extracellular vesicles implanted by mineralising osteoblasts into the collagenous matrix which control nucleation of the first mineral crystals. MVs are hypothesised to accumulate amorphous calcium phosphate (ACP) prior to mineral nucleation, regulated by phosphatases including PHOSPHO1 and TNAP. However, the biochemical and physiochemical mechanisms which control ACP generation and trigger crystal formation remain unclear.

Purpose: This novel toolkit aims to use physical chemistry approaches to enable investigation of MV biology.

Methods: MC3T3-E1 mouse osteoblasts were plated in Ibidi dishes and mineralised in osteogenic media for 7 days. Cells were incubated with or without lansoprazole (PHOSPHO1 inhibitor; 10μM) or levamisole (TNAP inhibitor; 50μM) and with with 100μM propargyl choline for 24h prior to fixation.

The alizarin red assay was used to monitor matrix mineralisation. Biorthogonal incorporation of propargyl choline into the phospholipid phosphatidylcholine, and therefore cellular membranes, was detected using a click chemistry reaction with a fluorescent azide. Cell plasma membranes were stained using CellBrite Red and pseudo-super resolution confocal z-stacks acquired using a Leica Stellaris 5 microscope equipped with LIGHTNING processing. Cells were subsequently prepared for transmission electron microscopy (TEM) and examined using a Hitachi HT7800 at 100kV.

Results: Inhibition of PHOSPHO1 or TNAP significantly reduced matrix mineralisation ($p < 0.05$). Pseudo-super resolution microscopy revealed successful biorthogonal labelling of cellular membranes using propargyl choline and enabled detection of small extracellular particles surrounding cells. Extracellular particles appeared to increase with phosphatase inhibition. Correlated TEM revealed these particles to be membrane-bound MVs embedded in collagenous matrix and containing electron-dense material.

Conclusions: Biorthogonal labelling of phosphatidylcholine lipids using propargyl choline can successfully label MVs as detected using click chemistry. MV breakdown and mineral nucleation is repressed with inhibition of phosphatases. Future work will use solid state NMR to probe MV dynamics during ACP accumulation and mineral nucleation.

P199

Comparisons of thigh muscle fat content between quantitative CT (QCT) and chemical shift encoded MRI (CSE-MRI)

Wenshuang Zhang[1], Ling Wang[2], Yi Yuan[1], Xiaoguang Cheng[2]
[1]Beijing Jishuitan Hospital- Peking University Fourth School of Clinical Medicine, Department of Radiology, Beijing, China
[2]Beijing Jishuitan Hospital, Department of Radiology, Beijing, China

Abstract Text

Introduction: This study evaluated the correlation and consistency of quantitative CT (QCT) and chemical shift encoded MRI (CSE-MRI) for quantifying thigh muscle fat content in healthy people and patients undergoing dialysis. QCT exhibited good correlation and consistency with CSE-MRI for thigh muscle fat quantitative measurements indicating that QCT may be a reliable alternative to CSE-MRIin clinical assessment of thigh muscle fat infiltration.

Purpose: To compare the agreement and correlation of measurements of thigh muscle fat content between QCT with CSE-MRI in both healthy people and patients undergoing dialysis.

Materials and methods: 28 healthy individuals and 28 dialysis patients underwent thigh QCT and CSE-MRI examinations. The CT fat fraction (CTFF) and MR proton density fat fraction (PDFF) values of left quadriceps femoris were measured at the level of the mid-upper thigh. CTFF and PDFF were plotted as histograms. Scatterplots, Bland-Altman plots and Spearmen correlation coefficients were used to examine the relationship between CTFF and PDFF. The comparisons between CTFF and PDFF were investigated by the *Wilcoxon* signed rank test. The comparisons of CTFF or PDFF between the healthy group and dialysis group were also investigated by the *Wilcoxon* signed rank test.

Results: CTFF of left quadriceps femoris was positively correlated with PDFF in all subjects (r_s=0.83, $P<$ 0.001). Bland-Altman analysis revealed good agreement between CTFF and PDFF, with an average difference in left quadriceps femoris of 0.09%. The difference between CTFF and PDFF of left quadriceps femoris was statistically insignificant (*P*=0.78). The difference of CTFF or PDFF between the healthy group and dialysis group was statistically significant (*P*=0.02, 0.03, respectively).

Conclusion: QCT exhibited good correlation and consistency with the CSE-MRI method in quantifying thigh muscle fat content. In the future, QCT could serve as a reliable tool for quantitative analysis of thigh muscle fatty infiltration among patients undergoing dialysis.

P204

PHOSPHO1-MNeonGreen expressing osteoblasts allow high resolution imaging of matrix vesicles during the early stages of in vitro mineralisation

Charlotte Clews[1], Scott Dillon[2], Fabio Nudelman[3], Louise Stephen[1], Colin Farquharson[1]
[1]The University of Edinburgh, The Roslin Institute, Edinburgh, United Kingdom
[2]The University of Cambridge, The department of Chemistry, Cambridge, United Kingdom
[3]The University of Edinburgh, The department of Chemistry, Edinburgh, United Kingdom

Abstract Text

Background: Bio-mineralisation is an essential process initiated by osteoblasts and chondrocytes involving calcium phosphate crystal deposition within the collagenous extracellular matrix to form an organic-inorganic composite material that is both tough and stiff. The delicate balance of inorganic phosphate and pyrophosphate concentrations is a major determinant of the rate of mineralisation, and is under the control of tissue non-specific alkaline phosphatase (TNAP) and PHOSPHO1, key phosphatases involved in matrix vesicle (MV) driven mineralisation. MVs are small (50 - 300 nm) spherical bodies that concentrate calcium and phosphate leading to the delivery and deposition of amorphous calcium phosphate or hydroxyapatite onto the collagen scaffold. Numerous theories have been proposed for the bio-molecular basis of MV production with links to the actin cytoskeleton and small GTPases.

Purpose: To establish the mechanisms underpinning MV formation using novel super-resolution fluorescence imaging technologies, and the role of MVs in skeletal mineralisation by chondrocytes and osteoblasts.

Methods: Mineralisation timecourses used qPCR, western blotting to ascertain gene and protein expression during in-vitro mineralisation. Fluorescent plasmid constructs containing PHOSPHO-1 tagged with small fluorescent protein mNeonGreen were transfected into MC3T3 C14, followed by high resolution fixed and live confocal imaging.

Results: Mineralisation timecourses of MC3T3 (osteoblast-like cells) and ATDC5 (chondrocyte-like cells) show mineralisation after days 9 and 20 respectively, an increase in PHOSPHO1 and TNAP and a decrease in Col1α1 expression. Fixed imaging shows evidence of intracellular trafficking and extracellular release of small, vesicular objects of MV size, positive for PHOSPHO1. Further work shows cytoskeletal involvement in vesicle production and release, and confirmation of actin, vimentin and vinculin in focal adhesion-like formations at release sites. Live cell imaging was confirmatory, showing vesicle movement along filamentous protrusions from the membrane, co-localising with filamentous actin.

Conclusion: PHOSPHO1-MnG is a suitable model for visualising MVs in the early stages of in vitro mineralisation.

P212

The role of iron and the iron sensor transferrin receptor 2 (Tfr2) in heterotopic ossification

Sven Spangenberg[1], Lorenz Hofbauer[1], Martina Rauner[1], Ulrike Baschant[1]
[1]Technische Universität Dresden Medical Center,
Department of Medicine III and Center for Healthy Aging, Dresden, Germany

Abstract Text

Overview
Heterotopic ossification (HO) is bone formation at abnormal anatomical sites, developing in three main stages: inflammation, chondrogenesis and osteogenesis. Bone morphogenetic protein (BMP) signaling plays an important role in the pathogenesis of HO and is also an important regulator of iron homeostasis. The iron sensor transferrin receptor 2 (Tfr2) regulates iron cell uptake, but also bone formation.

As $Tfr2^{-/-}$-mice are iron overloaded and show enhanced HO, we aimed to investigate the impact of iron levels and the cell-intrinsic role of Tfr2 on HO development.

Methods
HO was induced in *$Tfr2^{-/-}$*-mice and wild-type littermates and in mice lacking the Tfr2 in myeloid cells ($Tfr2^{LysMCre}$) or osteoblasts ($Tfr2^{OsxCre}$) by injection of recombinant BMP-2 into the M. tibialis anterior. In addition, wild-type mice were fed with a high iron (25,000 ppm Fe) or low iron diet (<10 ppm Fe) for 8 weeks starting from weaning before HO was induced. The HO sites were analyzed by flow cytometry (day 2) and µCT analysis (day 14).

High iron diet in WT mice led to a 34-fold increase in HO 14 days after BMP-2 injection ($p<0.001$), while low iron diet led to a huge decrease (55.16 to 0.61 mm^3 BV, $p<0.05$).
After subjecting $Tfr2^{LysMCre}$-mice to HO, there was no difference to controls, but interestingly, Tfr2 deletion in osteoblasts ($Tfr2^{OsxCre}$-mice) led to more HO progression than littermate controls (2-fold increase, $p<0.05$).
Analyzing the inflammatory phase of HO in $Tfr2^{-/-}$-mice, we found no strong difference in the frequency of CD45+ hematopoietic or CD11b+GR1+ myeloid cells, but the inflammatory macrophages were higher (21.10 vs 39.90 % of CD45+ cells, $p<0.05$).

Conclusion
Iron levels as well as the iron regulator Tfr2 in Osx-expressing osteoprogenitor cells affect the development of HO, most likely already at the early inflammatory stage of HO by increasing the fraction of inflammatory macrophages.

P285

DXA-derived knee shape is associated with knee osteoarthritis, knee pain and knee replacement: findings from a study of 37,924 people in UK Biobank.

Rhona Beynon[1], Fiona Saunders[2], Raja Ebsim[3], Monika Frysz[1,4], Jenny Gregory[2], Claudia Lindner[3], Richard Aspden[2], Nicholas Harvey[5], Timothy Cootes[3], Jon Tobias[1,4]
[1]University of Bristol, Musculoskeletal Research Unit- Bristol Medical School, Bristol, United Kingdom
[2]University of Aberdeen, The Institute of Medical Sciences, Aberdeen, United Kingdom
[3]University of Manchester, Division of Informatics- Imaging & Data Sciences, Manchester, United Kingdom
[4]University of Bristol, Medical Research Council Integrative Epidemiology Unit, Bristol, United Kingdom
[5]University of Southampton, MRC Lifecourse Epidemiology Centre, Southampton, United Kingdom

Abstract Text

Background:

Knee osteoarthritis (kOA) is a degenerative joint disease affecting the whole of the joint. Statistical shape modelling (SSM) of knee x-ray images and magnetic resonance images suggest that specific shape modes (SMs) may be associated with kOA. No large-scale studies have applied SSM to knee dual-energy X-ray absorptiometry (DXA) scans.

Purpose

To assess relationships between knee shape derived from DXA scans using SSM, and kOA clinical outcomes.

Methods:

A 120-point SSM, comprising the femur, tibia, and fibula, was applied to knee DXA images obtained from the UKBiobank imaging enhancement study. Associations between the top 10 SMs (explaining 77% of variation in knee shape) and kOA outcomes, including hospital-diagnosed kOA (HES-kOA), knee pain, and knee replacement, were examined using logistic regression (adjusted for age, sex, height, and weight). We report odds ratios (OR) with 95% confidence intervals (CI) for each standard deviation increase in SM. Composite at-risk shapes were plotted by combining SMs associated with the outcome of interest at a Bonferroni significant threshold of p-value <0.005.

Results:

Complete data were available for 37,924 participants (47.9% males). Mean age was 63.7 years (range 45-82 years). 5,596 participants (14.8%) reported pain, 1,557 (4.1%) had HES-kOA, and 438 (1.2%) had knee replacements. We identified four SMs associated with pain (2 [OR:1.07;CI:1.04,1.11], 5 [0.88;0.85,0.90], 6 [1.15;1.12,1.19] and 7 [1.06;1.03,1.10]), HES-kOA (5 [0.84;0.80,0.89], 6 [1.27;1.20,1.33], 8 [0.90;0.85,0.95] and 10 [0.92;0.88,0.97]), and knee replacement (4 [0.86;0.78,0.95], 5 [0.76;0.69,0.84], 6 [1.51;1.37,1.66] and 10 [0.81;0.74,0.90]). Composite SMs visualising the combined

adjusted associations indicate varus alignment, medial joint space narrowing, and protrusion of the lateral aspect of the distal femur (Figure 1).

Conclusions:

DXA-derived knee shape showed expected associations with clinical kOA outcomes, namely increased varus alignment of femur and tibia and medial joint space narrowing. Further studies are planned to evaluate the utility of knee DXA scans in early detection of knee OA.

Figure 1: Composite shape models visualising the combined adjusted associations of shape modes with kOA outcomes.

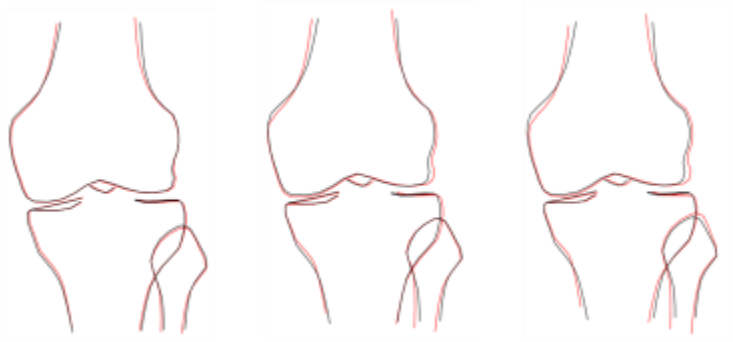

Black lines represent the SSM mean Knee shape. Red lines represent the composite at-risk shapes.

BRS Only Poster Abstracts

P001

Characterisation of osteosarcoma cell matrix signatures reveals nanoscale molecular composition is linked to pro-angiogenic potential.

Aikta Sharma[1], *Richard Oreffo*[2], *Sumeet Mahajan*[3], *Stephen Beers*[4], *Janos Kanczler*[2], *Claire Clarkin*[5]
[1]*University College London, Mechanical Engineering, London, United Kingdom*
[2]*University of Southampton, Institute of Developmental Sciences, Southampton, United Kingdom*
[3]*University of Southampton, Chemistry, Southampton, United Kingdom*
[4]*University of Southampton, Cancer Sciences, Southampton, United Kingdom*
[5]*University of Southampton, Biological Sciences, Southampton, United Kingdom*

Abstract Text

Background. A defining feature of osteosarcoma (OS) is the synthesis of a pathological extracellular matrix (ECM) that is accompanied by a dedicated tumour vascular network, both of which critically support metastatic progression. This study focused on determining whether the ECM signatures OS cell lines are distinct from osteoblasts (OBs) by grade, and whether cell-specific matrices couple to angiogenic potential.

Methods. OS cell lines, Saos-2 (low-metastatic grade) and 143B, (high-metastatic grade) were cultured for up to 14 days *in vitro*. Raman spectroscopy was performed on individual OS cells (N=25) to characterise OS-ECM composition and compared to OB-ECM (MC3T3) signatures. Angiogenic and osteogenic differentiation status was performed in parallel by quantification of VEGF release by ELISA and enzymatic alkaline phosphatase (ALP) assays, respectively.

Results. Raman spectroscopy revealed elevations in collagen-specific proline of the OS-ECM were exclusive to 143B cultures ($P=0.007$) on day 14, versus MC3T3s. Grade-specific distinctions in immature (amorphous calcium phosphate, ACP) and mature (carbonated apatite, CAP) precursors of hydroxyapatite were evident with low ACP (day 1 and day 4, $P<0.0001$; day 14, $P=0.04$) and high CAP (day 1, day 4 and day 14, $P<0.0001$) in Saos-2 cultures and high ACP (day 4 and day 14, $P<0.0001$) and low CAP (day 1, day 4 and day 14, $P<0.0001$) in 143B cultures versus MC3T3s. This correlated with elevated ALP activity in Saos-2 cultures across all time-points (day 1, $P=0.0001$; day 4 and day 14, $P<0.0001$) versus MC3T3s. VEGF release was elevated on day 1 ($P=0.001$) in Saos-2 cultures and day 4 ($P<0.0001$) and on day 14 in 143B cultures ($P<0.0001$) versus MC3T3s.

Conclusions. The ECM signatures of OS are distinguishable from OBs by grade and linked to distinct angiogenic and osteogenic differentiation profiles. Our data suggests that such ECM signatures can be used to report metastatic potential in a diagnostic and prognostic capacity.

P002

Oestrogen has a protective effect on chondrosarcoma growth in vitro and in vivo

Karan Shah[1], *Dionne Wortley*[2], *Lee Jeys*[2], *Alison Gartland*[1]
[1]*The University of Sheffield, Oncology and Metabolism, Sheffield, United Kingdom*
[2]*Royal Orthopaedic Hospital, Knowledge Hub, Birmingham, United Kingdom*

Abstract Text

Chondrosarcoma is the most common primary bone cancer (PBC) in adults and is responsible for greatest number of new cases of PBC. Relatively little is known about the aetiology of chondrosarcoma nor why a low-grade tumour de-differentiates, greatly reducing the 5-year survival rate to 29%. Chondrosarcoma affects men more than women (ratio1.5:1) and recent clinical data suggests that women have improved survival compared to men of comparable age. This effect diminishes after menopause, suggesting that oestrogen may have a protective effect in chondrosarcoma. In this study, we investigate the effects of oestrogen on human SW1353 chondrosarcoma cell proliferation and migration *in vitro* and on tumour growth *in vivo*.

The *in vitro* experiments were performed in oestrogen deplete conditions with exogenous oestrogen supplemented at varying concentrations (0-500nM). Cell proliferation was measured following oestrogen treatment for 72hr using WST-1 reagent and cell migration was assessed over 24hr using 'scratch' assays. SW1353 cell proliferation was 80% lower in oestrogen containing culture conditions compared to deplete conditions ($P<0.0001$) and addition of exogenous oestrogen (>10nM) to the deplete conditions lowered cell proliferation by 21% ($P<0.05$). Oestrogen reduced SW1353 cell migration in a dose-dependent manner with significant reduction observed for doses of 10nM and above ($P<0.05$).

For the *in vivo* study, 7-week old female NOD-scid gamma mice were subjected to ovariectomy (OVX), to mimic post-menopausal status, or sham-operated. One week post-surgeries, mice were injected with $2.5x10^5$ luciferase-expressing SW1353 cells sub-cutaneously and tumour burden monitored via bioluminescence imaging. At day 31, higher tumour burden was observed in the OVX mice compared to the sham controls ($1.53x10^6$ vs $6.76x10^5$; $P<0.0001$).

These preliminary data indicate that oestrogen plays a protective role in the progression of chondrosarcoma and are consistent with the clinical findings. A more comprehensive investigation is warranted to test the therapeutic potential of oestrogen supplementation in chondrosarcoma.

P003

Evidence for altered osteocyte morphology proximal to myeloma bone disease using synchrotron radiation micro-CT imaging

Rebecca Andrews[1], *Holly Evans*[1], *Jacob Trend*[2], *Goran Lovric*[3], *Claire Clarkin*[2], *Michelle Lawson*[1]
[1]*University of Sheffield, Oncology and Metabolism, Sheffield, United Kingdom*
[2]*University of Southampton, Developmental and Skeletal Biology, Southampton, United Kingdom*
[3]*Paul Scherrer Institut, Photon Science Division, Villigen, Switzerland*

Abstract Text

Myeloma is a blood cancer in which up to 90% of patients develop bone disease, resulting in osteolytic lesions, reduced bone mineral density and trabecular thinning. These changes cause pain, immobility, and risk of fracture. The impact on quality of life for patients is significant and there is an unmet clinical need to develop better treatments. Historically, it has not been possible to properly assess or quantify osteocyte lacunae, as its visualisation requires sub-micron resolution. Recently we acquired access to the Swiss Light Source (Paul Scherrer Institute, Switzerland) to obtain high-resolution synchrotron radiation micro-CT images of long bones from mice with myeloma bone disease (MBD) and controls. We hypothesised that osteocyte lacunae are significantly altered in myeloma-bearing bones compared to non-tumour controls, potentially contributing to bone destruction. We scanned long bones of both synergic (5TGM1) and xenograft (U266) models of myeloma at a resolution of 0.65um², allowing us to visualise osteocyte lacunae using Dragonfly. By comparing tumour mice to naïve controls, we were able to show that osteocyte parameters remained similar at the tibiofibular junction, a region far from osteolytic disease – osteocyte density was 56816 ± 5429/mm³ in diseased bone vs 58819 ± 9190/mm³ in naïve bone; and average osteocyte volume was 110.1 ± 12.0 um³ vs 172.0 ± 122.2um³. However, in a region close to osteolytic disease at the growthplate, we showed that osteocyte density decreased but volume increased – osteocyte density was 6143 ± 1231/mm³ in diseased bone vs 14346 ± 2417/mm³ in naïve bone; osteocyte volume was 385.5 ± 31.2um³ vs 185.8 ± 12.1mm³. In summary, we observed changes in the density and volume of osteocyte lacunae in areas of established osteolytic lesions compared to non-MBD regions, raising questions as to the role of osteocytes in myeloma and the potential for them to be targeted therapeutically.

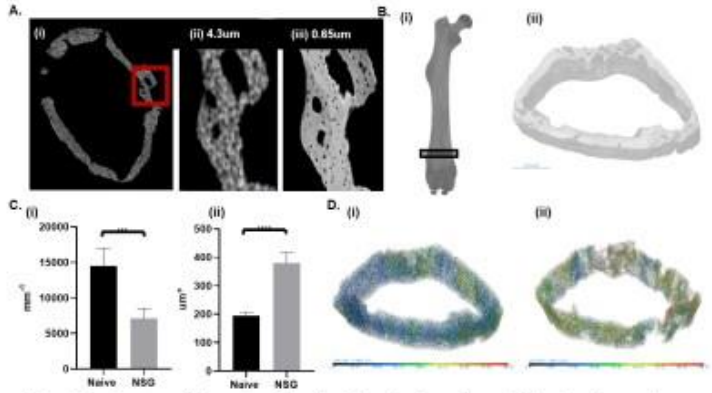

Figure 1. Synchrotron radiation micro-CT imaging of myeloma bone disease. (A) Imaging of a mouse femur, with (i) a cross-sectional image with the red highlighted region then scanned on (ii) a benchtop micro-CT scanner at 4.3µm and (iii) using synchrotron radiation micro-CT (SRCT) at 0.65µm. (B) 3-d rendering of of (i) scanned femur and (ii) the region analysed (C) Femoral analysis in naïve and NSG mice of (i) osteocyte density and (ii) osteocyte volume. (D) Representative 3-D images showing osteocyte volume for (i) naïve and (ii) NSG mice.

P004

Monitoring breast cancer-induced bone disease in nude mice using in vivo µCT

Yue Chun Jacky Wong[1], *Lubaid Saleh*[2], *Holly R. Evans*[2], *Enrico Dall'Ara*[3], *Michelle A. Lawson*[2], *Ingunn Holen*[2]
[1]*Univesity of Sheffield, Oncology and metabolism, Sheffield, China*
[2]*University of Sheffield, Oncology and metabolism, Sheffield, United Kingdom*
[3]*University of Sheffield- INSIGNEO Institute for in silico Medicine, Oncology and metabolism, Sheffield, United Kingdom*

Abstract Text

Background: Breast cancer-induced bone disease is a result of localised lytic bone lesions that cause bone fragility and pain. Previous studies have mainly used *ex vivo* µCT to investigate the end-stage effects of breast tumour growth in bone. We investigated whether *in vivo* µCT, combined with bioluminescence imaging of tumour burden, can be used to detect the formation and map the development of breast cancer-induced bone lesions in nude mice.

Methods: 6-week-old female BALB/c nude mice were injected (intra cardiac) with $5x10^5$ Luc2+ve MDA-MB-231 cells (n=10). Tumour growth was monitored by bioluminescence imaging twice weekly, left proximal tibiae and distal femora were scanned by *in vivo* µCT once weekly (VivaCT80 µCT scanner) and by *ex vivo* µCT at endpoint.

Results: Tumours developed in hind limbs of all mice by week 2 after tumour injection, with tumour burden increasing up to 4 weeks. No soft tissue tumour growth was detected. *In vivo* µCT demonstrated that lytic lesions appeared in the tibia 1 week after tumour injection and in the femur after 3 weeks, with large lesions established in either the tibia or the femur after 4 weeks. In both tibia and femur, trabecular BV/TV (%), trabecular number (mm^{-1}) and trabecular thickness (mm) were decreased 1 week after tumour injection compared to baseline, this decrease continued over the following 3 weeks (Table 1). *Ex vivo* µCT results (BV/TV (%)) agreed with the *in vivo* µCT results at week 4. Taken together, trabecular BV/TV (%) decreased as tumour burden increased.

Conclusion: Our results support that *in vivo* µCT can be used to track the development of lytic bone lesions from the very early stages of breast cancer-induced bone disease.

Table 1. Left hindlimb bone parameters detected by weekly *in vivo* µCT

	Percentage bone volume (BV/TV)		Trabecular thickness (Tb.th)		Trabecular number (Tb.N)	
	Tibia					
Week	Mean	*P*	Mean	*P*	Mean	*P*
0	4.651		0.034		4.55	
1	4.226	*,0.0137	0.032	0.4646	2.181	****,<0.0001
2	3.443	****,<0.0001	0.027	****,<0.0001	1.27	****,<0.0001
3	2.14	****,<0.0001	0.028	****,<0.0001	0.654	****,<0.0001
4	1.693	****,<0.0001	0.025	****,<0.0001	0.42	****,<0.0001
	Femur					
Week	Mean	*P*	Mean	*P*	Mean	*P*
0	6.076		0.034		2.456	
1	5.328	****,<0.0001	0.032	0.4646	2.42	0.9932
2	4.626	****,<0.0001	0.027	****,<0.0001	1.433	****,<0.0001
3	4.014	****,<0.0001	0.028	****,<0.0001	1.144	****,<0.0001
4	3.135	****,<0.0001	0.025	****,<0.0001	0.816	****,<0.0001

& ** significant compared to week 0 baseline (before tumour cell injection)*

P005

Targeting dormant myeloma cells using standard of care therapies

Hawazen Algifry[1], *Georgia Stewart*[2], *Darren Lath*[1], *Jennifer Down*[1], *Alexandria Sprules*[1], *Munitta Muthana*[1], *Michelle Lawson*[1]
[1]*University of Sheffield, Oncology & Metabolism, Sheffield, United Kingdom*
[2]*University of Sheffield, Oncology and Metabolism, Sheffield, United Kingdom*

Abstract Text

Background: Multiple myeloma is caused by abnormal plasma cell growth in the bone marrow and disease reoccurrence post chemotherapy is common. It has been speculated that dormant myeloma cells (DMCs) that residue in endosteal bone niches play a role in disease relapse due to their drug resistance. Therefore, we aimed to assess the efficacy of standard of care (SoC) anti-myeloma therapies on DMCs. We hypothesise SoC anti-myeloma therapies when used in combination can target DMCs more effectively than single therapies.

Methods: Four myeloma cell lines (murine 5TGM1, and human JJN3, OPM2, U266 transduced with GFP and Luc) were labelled with a vybrant membrane dye 1,1'-dioctadecyl-3,3,3',3'-tetramethylindodicarbocyanine (DID) to track DMCs over 21 days of culture using fluorescent microscopy and flow cytometry. Cell populations were treated with different concentrations of SoC therapies (bortezomib, melphalan, and panobinostat) to determine IC_{50} values on cell viability after 3 and 5 days of culture using an alamarBlue™ asssay.

Results: Fluorescent microscopy and flow cytometry demonstrated the presence of DID-labelled cells (DID^{high}: potential DMCs, DID^{low}: slow growing MCs, and $DID^{negative}$: proliferating cells) and these declined over time in all cell lines. DID^{high} cells were observed in 5TGM1 (0.1%) and JJN3 (0.2%) cultures at 17 days, by day 21 <0.1% DID^{high} cells were detected. For OPM2 cells, no DID^{high} cells were detected after 10 days. The IC_{50} values of SoC therapies were determined (bortezomib 0.58-1.93nm, melphalan 0.54-4.98nm, and panobinostat 0.36-13.37nm).

Conclusions: In summary, we have demonstrated for the first time the presence of DMCs in cultures JJN3 cells. We have determined drug IC50 values in 4 cell lines and these will be used in future *in vitro* and *in vivo* studies to determine their efficacy on DMCs when used alone or in combination.

P011

Establishment and characterisation of a human osteosarcoma metastatic cell line derived from a patient's lung for future preclinical use

Luke Tattersall[1], *Victoria Tippett*[1], *Adrian Higginbottom*[2], *Juha K Rantala*[3], *Alison Gartland*[1]
[1]*The University of Sheffield, Oncology & Metabolism, Sheffield, United Kingdom*
[2]*The University of Sheffield, Sheffield Institute for Translational Neuroscience SITraN, Sheffield, United Kingdom*
[3]*Misvik Biology, Misvik Biology, Oy- Turku, Finland*

Abstract Text

Osteosarcoma is the most common type of primary bone cancer affecting children/adolescents. It is a rare incurable often-fatal disease with metastasis most commonly occurring in the lungs. This results in an extremely poor prognosis and reduced 5-year survival rate of 20% compared to 60% when the disease is localised. Representative models for rare cancers are limited, with osteosarcoma human cell lines being derived from the primary bone tumour and have been used in culture for half a century. There is an absence of pre-clinical metastatic models hindering our understanding of disease progression.

We have developed a newly isolated cell line (MISB166) derived from a high grade osteoblastic osteosarcoma patient directly from the lung metastasis and performed characterisation *in vitro.* We have determined the growth rate, migration and sensitivity to standard of care MAP chemotherapy of MISB166 (as resistance frequently occurs in patients and reduces survival).

MISB166 was found to have a doubling time of 83-106 hours based on enzymatic WST-1 assays and cell counting. It possesses a chemoresistant phenotype compared to established osteosarcoma cell lines (100µM-0.003µM dose range, see table below). When assessing which chemotherapy was the most effective, MISB166 was most sensitive to doxorubicin, followed by cisplatin and methotrexate.

Our future work will involve *in vivo* studies to determine if MISB166 can be used as a metastatic osteosarcoma model using both paratibial and intracardiac injection techniques in immunocompromised mice.

In conclusion, we have established MISB166 as a chemoresistant metastatic osteosarcoma cell line with potential utility to investigate mechanisms of and new treatments for chemoresistance and metastasis in osteosarcoma.

Cell Line	Doxorubicin IC_{50}	Cisplatin IC_{50}	Methotrexate IC_{50}
143B	79nM	3.55µM	706nM
TE85	240nM	7.09µM	7.52µM
SaOS-2	316nM	12.27µM	10.05µM
MISB166	5.12µM	15.81µM	26.65µM

P012

Osteoblastic and adipogenic precursor cell population in a mouse model of chronic kidney disease

Worachet Promruk[1], *William Cawthorn*[2], *Katherine Staines*[3], *Louise Stephen*[1], *Colin Farquharson*[1]
[1]*The Roslin Institute, University of Edinburgh, Edinburgh, United Kingdom*
[2]*The Queen's Medical Research Institute, University of Edinburgh, Edinburgh, United Kingdom*
[3]*School of Pharmacy & Biomolecular Sciences, University of Brighton, Brighton, United Kingdom*

Abstract Text

Chronic kidney disease (CKD) is a progressive and irreversible disease resulting in the loss of kidney function. This leads to altered calcium and phosphorous homeostasis and bone loss, commonly referred to as renal osteodystrophy (ROD). Previous studies have reported an increase of bone marrow adipose tissue (BMAT) in clinical and animal models of CKD but the mechanisms driving BMAT accumulation are unclear. This study assessed skeletal stem cells (SSC), osteoblastic (OPC) and adipogenic (APC) precursor cell populations, and osteoclast and osteoblast number in a mouse model of ROD. Eight-week-old male C57BL/6 mice received a diet supplemented with 0.2% adenine for up to 5-weeks to induce CKD. Control mice received the same diet without adenine. Serum analytes were quantified by ELISA and a biochemistry analyser. Precursor cell populations in bone marrow were quantified by flow cytometry and osteoclast and osteoblast number/bone surface were determined by bone histomorphometry. CKD development in mice was confirmed by elevated serum levels of creatinine, BUN, PTH and FGF-23. SSC as a % live single cells was reduced in CKD but there % of CD45- & CD31- cells was unchanged from control mice. The number of OPC as a % of live single cells, CD45- & CD31- cells and SSC were all higher in CKD mice than in control mice whereas the number of APC was unchanged. In CKD mice, osteoblast number was decreased at 5 weeks whereas osteoclast number was increased from 1 week in CKD mice. These flow cytometry data were unexpected but the expansion of BMAT in CKD may be a consequence of the rapid differentiation of adipocytes from APCs and/or the transdifferentiation of OPCs to the adipocyte lineage. Ongoing studies will determine the differentiation potential of adipocytes and osteoblasts from their common precursors during CKD and ROD development.

P013

Withdrawn

P014

The rebirth of tetracyclines: In vitro and ex vivo evaluation of osteogenic capabilities of Sarecycline

Victor Martin[1,2], *Liliana Grenho*[1,2], *Maria Helena Fernandes*[1,2], *Pedro Gomes*[1,2]
[1]*Faculty of Dental Medicine- University of Porto, Laboratory for Bone Metabolism and Regeneration, Porto, Portugal*
[2]*LAQV/REQUIMTE, University of Porto, Porto, Portugal*

Abstract Text

Background: Tetracyclines (TCs) embrace a class of broad-spectrum antibiotics with unrelated effects at sub-antimicrobial levels, including an effective anti-inflammatory activity and stimulation of osteogenesis, allowing their repurposing for different clinical applications. Recently, Sarecycline (SA) - a new-generation molecule with a narrower antimicrobial spectrum - was clinically approved due to its anti-inflammatory profile and reduced adverse-effects verified with prolonged use. Notwithstanding, little is known about its osteogenic potential, previously verified for early generation TCs.

Purpose/Methods: Accordingly, the present study is focused on the assessment of the response of human bone marrow-derived mesenchymal stromal cells (hBMSCs) to a concentration range of SA, addressing the metabolic activity, morphology and osteoblastic differentiation capability, further detailing the modulation of Wnt, Hedgehog and Notch signaling pathways. In addition, an *ex vivo* organotypic bone development system was established in the presence of SA and characterized by microtomographic and histochemical analysis.

Results: hBMSCs cultured with SA presented a significantly increased metabolic activity compared to control, with an indistinguishable cell morphology. Moreover, RUNX2 expression was upregulated 2.5-folds, and ALP expression was increased around 7-folds in the presence of SA. Further, GLI2 expression was significantly upregulated ($p < 0.05$), while HEY1 and HNF1A were downregulated, substantiating Hedgehog and Notch signaling pathways' modulation. The *ex vivo* model developed in the presence of SA presented a significantly enhanced collagen deposition, extended migration areas of osteogenesis, and an increased bone mineral content, substantiating an increased osteogenic development.

Conclusion: Summarizing, sarecycline is a promising candidate for drug repurposing within therapies envisaging the enhancement of bone healing/regeneration.

P016

Femoral Geometry in Bisphosphonate-related Atypical Femoral Fracture and Bisphosphonate-naïve Atypical Femoral Fracture

Wachirawit Songsantiphap[1], *Atiporn Therdyothin*[1], *Tanawat Amphansap*[1]
[1]*Police General Hospital, Department of orthopedics, bangkok, Thailand*

Abstract Text

Backgrounds: Atypical femoral fracture (AFF) was related, but not restricted to prolonged bisphosphonate (BP) use with possibly different femoral geometry between BP-related AFF (BPAFF) and BP-naïve AFF (BPnAFF)

Objectives: To compare radiographic characteristics of femoral geometry in BPAFF and BPnAFF

Methods: A retrospective cohort study was performed at Police General Hospital, Thailand, from January 2012 to December 2022. Medical records and all available radiograph of hip and femoral fractures were reviewed. AFFs were defined using criteria by American Society for Bone and Mineral Research (ASBMR). BPAFF were identified in patients with longer than two years of BP prescription. Femoral offset, neck shaft angle and lateral cortical thickness (LCT) index were compared between BPAFF and BPnAFF.

Results: A total of 13 BPAFF and 10 BPnAFF were identified. BPAFF patients were younger (73.46±6.30 vs 82.6±3.71 years, p<0.001). Localized periosteal thickening was more prevalent in BPAFF (7(30.43%) vs 1(4%), p = 0.074). Fractures were more prevalent in subtrochanteric region in BPAFF group (13(56.52%) vs 10(43.48%), p=0.04). BPAFF group had significantly higher LCT index at subtrochanteric level (0.258±0.050 vs 0.211±0.067, p=0.037), and at femoral shaft level (0.357±0.056 vs 0.288±0.059, p=0.005). (Table 1)

Conclusions: BPAFF had a higher LCT index at subtrochanteric and femoral shaft level when compared to BPnAFF.

Table 1 Femoral geometry of atypical femoral fractures in Bisphosphonate-related Atypical Femoral Fracture (BPAFF) and Bisphosphonate-naïve Atypical Femoral Fracture (BPnAFF)

	Mean(SD) BPAFF	Mean(SD) BPnAFF	P-value
Femoral offset	3.1931(±0.828)	3.25(±0.668)	0.429
Femoral neck-shaft angle	139.138(±9.383)	141.47(±7.562)	0.264
Lateral cortical thickness index (Lesser trochanter)	0.1635(±0.029)	0.1513(±0.028)	0.165
Lateral cortical thickness index (Subtrochanter)	0.2581(±0.050)	0.2118(±0.067)	0.037
Lateral cortical thickness index (Shaft)	0.3579(±0.056)	0.2887(±0.0592)	0.005

P017

Preventing periprosthetic joint infection: evaluating a novel antimicrobial sol-gel approach

Sarah Boyce[1], *Christine Le Maitre*[2], *Tom Smith*[1], *Tim Nichol*[1]
[1]*Sheffield Hallam University, Biomolecular Sciences Research Centre, Sheffield, United Kingdom*
[2]*The University of Sheffield, Oncology and Metabolism, Sheffield, United Kingdom*

Abstract Text

Background/Introduction

Prosthetic joint infection (PJI) is a significant complication associated with 1-3% of arthroplasty procedures and the antimicrobial resistant, biofilm nature of these infections renders them a significant treatment challenge. Current prevention strategies include antibiotic bone cement; however, the recent decrease in its use means there is need for alternative, local antimicrobial delivery methods.

Purpose

This study evaluates performance of a novel silica-based, biodegradable sol-gel implant device coating as a localised antimicrobial delivery method.

Methods

Antimicrobial activity and biofilm reduction were assessed via disc diffusion and broth microdilution assays using the Calgary biofilm device and *Staphylococcus aureus* culture.

Cytotoxicity was evaluated using Alamar blue staining of primary bovine osteoblasts in the presence of tobramycin-containing sol-gel. Morphological changes of osteoblasts grown directly on sol-gel were visualised using DAPI and phalloidin staining. Quantification of tobramycin release from sol-gel coated titanium implant materials was measured by LC-MS.

Results

Antibiotic activity within sol-gel was shown to be comparable to antibiotics alone ($p< 0.05$). Tobramycin concentrations within sol-gel as low as 0.8 mg ml^{-1} inhibited *S. aureus* (MRSA) biofilm growth on coated peg-lids, a statistically significant effect upon biofilm reduction compared to untreated controls ($p<0.05$).

There was no significant difference ($p<0.05$) in metabolic activity between untreated and sol-gel exposed primary bovine osteoblasts, including antibiotic loaded sol-gel, indicating a lack of cytotoxicity, with exception of the maximum tobramycin concentration tested ($p= 0.0094$).

Conclusion

The ultrathin sol-gel coating shows low cytotoxicity, strong biofilm reducing activity and antimicrobial activity comparable to antibiotics alone; indicating potential as a local antimicrobial delivery system to inhibit PJI growth without the need for bone cement. Future work will develop and evaluate sol-gel

performance in an *ex vivo* explant bone infection model which will reduce the need for animal experimentation.

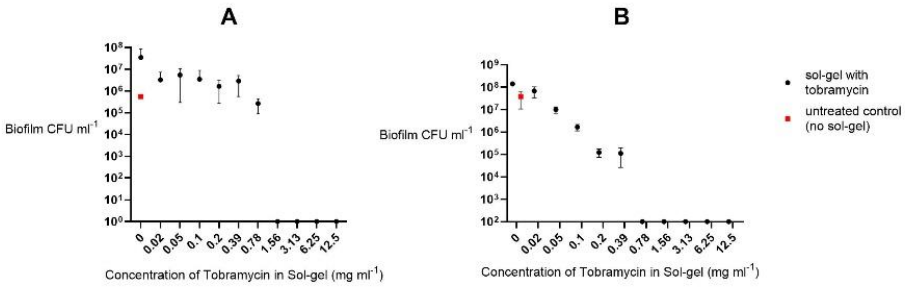

P018

The embryonic chicken femur organotypic culture as a new tool to evaluate the effects of hyperglycemia on bone metabolism and development

Rita Araujo[1,2], *Pedro Sousa Gomes*[1,2], *Maria Helena Fernandes*[1,2]
[1]*Faculty of Dental Medicine- University of Porto,*
BoneLab laboratory for bone metabolism and regeneration, Porto, Portugal
[2]*LAQV, ReQUIMTE, Porto, Portugal*

Abstract Text

Deleterious effects of Diabetes mellitus (DM) in different tissues and organs, including bone, are well described. Hyperglycemia seems to be one of the most contributing etiological factors of bone-related alterations, altering metabolic functionality and inducing morphological adaptations. Despite the established models for the assessment of bone functionality in hyperglycemic conditions, in vitro studies present limited representativeness given the restricted cell-cell and cell-matrix interactions, and three-dimensional spatial arrangement; while in vivo studies raise ethical issues and offer limited mechanistic characterization, given the modulatory influence of many systemic factors and/or regulatory systems.

This study aims to establish the influence of the hyperglycemic condition on bone tissue development, using the embryonic ex vivo chicken femur model. Thus, embryonic femurs of *Gallus domesticus* were obtained and cultured in organotypic air/liquid interface, for eleven days, in conditions that mimic hiperglycaemia, and three experimental groups were established GL12 (cultured in 12mM glucose medium), GL25 (cultured in 25mM glucose medium) and control.

Upon that time, samples were further analyzed. Results (refer to image) show that, despite the enhanced collagen production under the presence of high levels of glucose, structural discrepancies were verified, possibly related to the increased oxidative stress. Also, the mineralization process is severely impaired with subsequent alteration of bone's three-dimensional structure, as shown microtomographic analysis results (table, *p<0.05). Present study findings are coherent with previous *in vitro* and *in vivo* studies, therefore the ex vivo embryonic chicken femur shows potential as a tool to further screen the effects of hyperglycemic conditions on bone tissue metabolism and development.

	Control		GL12		GL25	
	Mean	*Stand.Dev.*	*Mean*	*Stand.Dev.*	*Mean*	*Stand.Dev.*
TotalVolume (mm^3)	22,36	1,63	52,85*	4,77	59,41*	1,10
BoneVolume (mm^3)	0,40	0,04	0,35	0,03	0,42	0,03
BV/TV (%)	1,79	0,11	1,39	0,37	0,69*	0,03
Cortical.Thickness (mm)	0.0662	0.0023	0.0429*	0.0034	0.0384*	0.0027

P019

3D mapping of the osteocyte lacunocanalicular and vascular network dynamics in ovariectomy-induced osteoporosis

Georgiana Neag[1], Oliver Aust[1], Daniela Weidner[1], Mareike Thies[2], Fabian Wagner[2], Mingxuan Gu[2], Sabrina Pechmann[3], Silke Christiansen[3], Andreas Maier[2], Stefan Uderhardt[4], Georg Schett[1]
[1]University Hospital Erlangen, Internal Medicine 3-Rheumatology and Immunology, Erlangen, Germany
[2]FAU Erlangen-Nürnberg, Pattern Recognition Lab, Erlangen, Germany
[3]Institute for Nanotechnology and Correlative Microscopy - INAM,
Fraunhofer Institute for Ceramics Technology and Systems - IKTS, Forchheim, Germany
[4]University Hospital Erlangen, University Hospital Erlangen, Erlangen, Germany

Abstract Text

Osteoporosis is a skeletal disease with a high prevalence in post-menopausal women, characterised by low trabecular and cortical bone mass and deterioration of bone microstructural integrity. These alterations render bones fragile and prone to fracturing, a state that has also been linked to the architectural and functional degradation of the intricate osteocyte lacunocanalicular network (LCN). However, the dynamics of the LCN metamorphosis during osteoporosis remain poorly understood to date, hampering development of interventions which prevent LCN degradation, to support maintenance of bone health. Here, we consecutively scanned murine tibiae collected from ovariectomised and control C57Bl6/N female mice (from day 4 up to 6 weeks post-surgery) to generate 3D maps of the tibia LCN and vascular network at both a cellular and geometric microscopic level. This was accomplished with the aid of lightsheet imaging and X-ray high-resolution microscopy and produced a detailed characterisation of LCN remodelling and vascular patterning in response to oestrogen depletion. Parameters generated focused on shape, density and alignment of the structures studied. Interestingly, striking changes were identified in the trabecular osteocyte lacunae shape (lacuna oblateness and stretch) in response to ovariectomy as early as 2-weeks post-surgery, a time-point that coincides with the trabecular bone mass loss identified by conventional micro-computed tomography (μ-CT) analysis. In conclusion, our data indicate that microscopic changes in the organisation of the LCN contribute to trabecular bone mass loss, arguing for the LCN as a target of ageing-related therapeutic focus.

P020

Efficacy of Plain Cholecalciferol Tablets vs. Ergocalciferol in Raising Serum Vitamin D Level in Thai Female Healthcare Workers

Tanawat Amphansap[1], Atiporn Therdyothin[1], Nitirat Stitkitti[1], Lertkong Nitiwarangkul[1], Vajarin Phiphobmongkol[1]
[1]Police General Hospital, Department of Orthopaedics, Bangkok, Thailand

Abstract Text

Abstract

Objectives

To compare the efficacy of cholecalciferol and ergocalciferol in raising 25-hydroxy vitamin D (25(OH)D) level in Thai female healthcare workers.

Methods

A randomized control trial was conducted in healthy female healthcare workers. Participants with previous vitamin D or calcium prescription, anti-osteoporotic treatment, medications or medical conditions affecting bone metabolism were excluded. Computer randomization allocated the participants into vitamin D2 group (n = 43), receiving ergocalciferol 20,000 IU weekly and vitamin D3 group (n = 40), receiving cholecalciferol 1,000 IU daily for 12 months. Venous blood sample was collected at baseline, 6 and 12 months for serum 25(OH)D, parathyroid hormone and calcium. Compliance was also assessed.

Results

The mean age of the participants was 50.6±9.9 and 50.9±8.4 years in vitamin D2 and D3 groups (P=0.884). The mean 25(OH)D levels were 16.91±6.07 ng/mL and 17.62±4.39 ng/mL (P = 0.547), respectively. Both groups had significant improvement in 25(OH)D level at 6 months (from 16.91±6.07 to 21.67±5.11 ng/mL and 17.62±4.39 to 26.03±6.59 ng/mL in vitamin D2 and D3 group). Improvement was significantly greater with cholecalciferol (P = 0.018). The level plateaued afterwards in both groups. (Figure 1) Only cholecalciferol could increase 25(OH)D in participants without vitamin D deficiency (6.88±4.20 ng/mL increment). Compliance was significantly better in vitamin D2 group (P = 0.025).

Conclusions

Daily cholecalciferol supplementation resulted in a larger increase in serum 25(OH)D level during the first six months comparing to weekly ergocalciferol. While vitamin D3 could increase serum 25(OH)D level in all participants, vitamin D2 could not do so in participants without vitamin D deficiency.

Figure 1 Serum 25-hydroxy vitamin D level in participants receiving vitamin D2 and vitamin D3

Figure 1 Serum 25-hydroxy vitamin D level in participants receiving vitamin D2 and vitamin D3

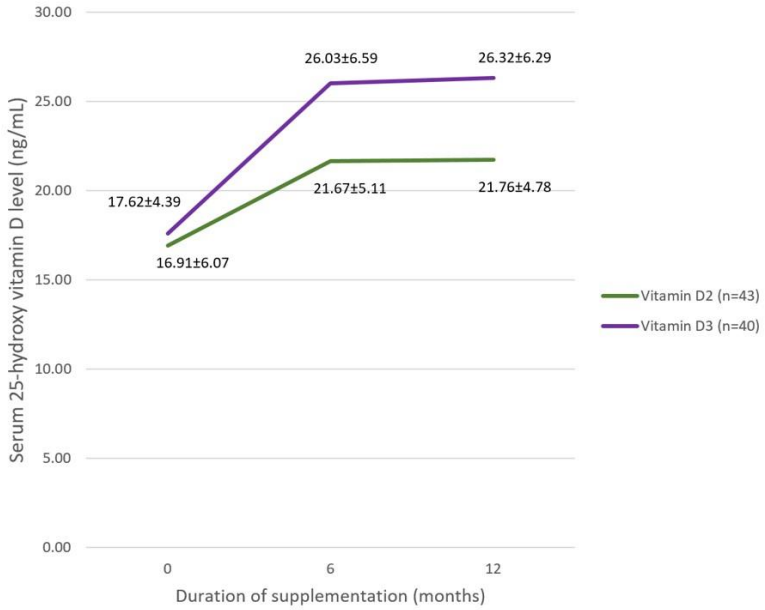

P021

"In vitro" characterization of gelatin-based haemostatic agents for bone tissue applications

Maria Guerra Gomes[1,2,3,4,5], *Liliana Grenho*[1,3], *Maria Helena Fernandes*[1,3], *Bruno Colaço*[3,4,5], *Pedro Gomes*[1,3]
[1]*Faculty of Dental Medicine of University of Porto,*
BoneLab - Laboratory for Bone Metabolism and Regeneration, Porto, Portugal
[2]*I3S – Institute for Research and Innovation in Health, Biocomposites, Porto, Portugal*
[3]*University of Porto, Requimte/LAQV, Porto, Portugal*
[4]*University of Trás-os-Montes and Alto Douro, CECAV - Animal and Veterinary Research Centre, Vila Real, Portugal*
[5]*University of Trás-os-Montes and Alto Douro,*
AL4AnimalS - Associate Laboratory for Animal and Veterinary Sciences, Vila Real, Portugal

Abstract Text

INTRODUCTION: The occurrence of bleeding following dental extraction is a relatively common complication, and topical haemostatic sponges are an important therapeutic option for its management when physiological processes are inefficient. These agents can remain at the site of application for up to 8 weeks, which could affect osteogenesis, thus making it important to assess their modulatory effects, and their leachables', on the alveolar bone.
PURPOSE: Given this, the aim of this study was the *in vitro* characterization of clinically available gelatin-based haemostatic agents (specifically, Hemospon®, Roeko® and Octocolagen®), in human osteoblastic cells.
METHODS: The haemostatic sponges' leachables were prepared in minimum essential medium (MEM), according to the ISO EN 10993-17 standard, and then added to human osteoblastic MG-63 cells, which were cultured in growth medium for 24 hours, at concentrations of 50% and 12,5%. A control group was cultured without leachables. The cell cultures were then assessed for cell viability and proliferation (metabolic activity (MTT) and DNA quantification), alkaline phosphatase (ALP) activity, mitochondrial and cellular morphology, as well as ALP histochemical staining and collagen content, at different timepoints.
RESULTS AND CONCLUSION: Data analysis revealed that cultures grown in the presence of distinct concentrations of the leachables were found to proliferate actively throughout the culture period, similarly to the control group, with minimal evidence of cell death or impaired cellular activity, and normal cellular morphology and collagen production. However, the Roeko® sponge induced a significantly higher ALP activity, in comparison to the other hemostatic agents' leachables, demonstrating to have some osteogenic potential, and suggesting a prospective application in bone tissue engineering-related approaches.

P022

An "in vitro" model to address canine periodontal regeneration

Laura Pinho[1,2,3,4,5,6,7], *André Queirós*[8], *Catarina Ferreira dos Santos*[6,7], *Bruno Colaço*[2,3,4,5], *Maria Helena Fernandes*[1,2]
[1]*Faculty of Dental Medicine- University of Porto,*
BoneLab - Laboratory for Bone Metabolism and Regeneration, Porto, Portugal
[2]*University of Porto, Requimte/LAQV, Porto, Portugal*
[3]*University of Trás-os-Montes and Alto Douro UTAD,*
Associate Laboratory for Animal and Veterinary Sciences AL4AnimalS, Vila Real, Portugal
[4]*University of Trás-os-Montes and Alto Douro UTAD, CECAV—Animal and Veterinary Research Centre, Vila Real, Portugal*
[5]*University of Trás-os-Montes and Alto Douro UTAD,*
CITAB - Centre for the Research and Technology of Agro-Environmental and Biological Sciences, Vila Real, Portugal
[6]*Higher Technical Institute, Centre for Structural Chemistry, Lisbon, Portugal*
[7]*Politechnic Institute of Setúbal, EST Setúbal- CDP2T, Setúbal, Portugal*
[8]*SCIVET, Group Breed, Paredes, Portugal*

Abstract Text
Background/Introduction: Dog's periodontal disease (PD) has a multifactorial etiology being a serious problem owing to its late diagnosis and high prevalence. Due to poor oral hygiene, and oral cavity size, the evolution from gingivitis to severe periodontitis is quick leading to progressive destruction of the tooth periodontal supporting tissues (gingiva, periodontal ligament and alveolar bone). The periodontal tissue is a complex connective tissue that include various cell types that interact to achieve the maintenance of all the tissues that compose the periodontium. Periodontal ligament stem cells (PDLSCs) are currently the most studied cell type in tooth-derived stem cells being easily isolated and differentiated into various types of cells including osteogenic cells, demonstrating an added value to be used in *in vitro* studies of the periodontal tissue.

Purpose: To establish an appropriate *in vitro* model to address canine periodontal regeneration.

Methods: Periodontal ligament was isolated from freshly extracted teeth from dog maxilla in a routine procedure, and explants were cultured in basal medium (α-MEM, 10% FBS, antibiotics, 37°C, 5% CO_2/air). PDLSCs (third passage) were cultured for up to 20 days in basal or osteogenic medium, and characterized for metabolic activity, total protein content and alkaline phosphatase (ALP) activity and cytochemical staining. Comparison of experimental conditions was assessed using the t-test and the one-way analysis of variance (ANOVA), followed by the post hoc Tukey.

Results: In basal and osteogenic-induced cultures, metabolic and alkaline phosphatase activities increased throughout the time and no significant differences were noted. However, osteogenic-induced cultures showed a cell layer organized in cellular clusters that stained intensely for ALP, contrasting to the continuous and homogeneous cell layer seen in basal conditions.

Conclusion: The possibility of modulating the behaviour of PDLSCs suggests its potential as an in vitro research model in canine periodontal regeneration helping to reduce animal use.

P023

Falciform ligament-derived mesenchymal stromal cells for bone regenerative applications

Carla Ferreira Baptista[1,2,3,4], *André Queirós*[5], *Rita Ferreira*[6], *Maria Helena Fernandes*[1,3], *Bruno Colaço*[4,7,8], *Pedro Sousa Gomes*[1,3]
[1]*Faculty of Dental Medicine- University of Porto,*
BoneLab - Laboratory for Bone Metabolism and Regeneration, Porto, Portugal
[2]*REQUIMTE/LAQV, Department of Chemistry University of Aveiro, Aveiro, Portugal*
[3]*University of Porto, Requimte/LAQV, Porto, Portugal*
[4]*University of Trás-os-Montes e Alto Douro UTAD, Centre for the Research and Technology of Agro-Environmental and Biological Sciences CITAB, Vila Real, Portugal*
[5]*SCIVET, grupo Breed, Paredes, Portugal*
[6]*University of Aveiro, REQUIMTE/LAQV- Department of Chemistry, Aveiro, Portugal*
[7]*University of Trás-os-Montes and Alto Douro, CECAV—Animal and Veterinary Research Centre UTAD, Vila Real, Portugal*
[8]*University of Trás-os-Montes and Alto Douro,*
Associate Laboratory for Animal and Veterinary Sciences AL4AnimalS, Vila Real, Portugal

Abstract Text

Introduction: Mesenchymal stromal cells (MSCs) are a relevant cell population for bone tissue regenerative approaches. These can be obtained from different sources such as bone marrow, umbilical cord/umbilical cord blood, adipose tissue, muscle, and periosteum. Regarding these, adipose tissue has been acknowledged as one of the most convenient sources of MSCs, due to the fact that they can be obtained in large quantities through minimally invasive procedures, and attain a high yield after isolation. In recent years, the falciform ligament (FL) has been reported as a potential depot for adipose tissue-derived stromal cells (FL-ADSCs) isolation, despite the absence of validated studies. That said, in the present study we have investigated the osteogenic capacity of this cell population, compared to that of ADSCs isolated from a control anatomical region, for prospective applications in bone regenerative medicine applications, using the dog as a model.

Methods: All experimental procedures were approved by the institutional ethics committee [15-CE-UTAD-2021]. Adipose tissue from FL and periovarian visceral region (control) was collected from 6 healthy dogs. ADSCs were isolated through an enzymatic dissociation process and cultured in the presence of osteogenic inducers. The obtained cultures were characterized at different periods for proliferation, morphology, and osteogenic activity. Comparison between groups was performed using analysis of variance and Tukey post-hoc test ($p < 0.05$).

Main Results: Our results demonstrated a significantly higher expression of osteogenesis-related genes, namely SOX9, RUNX2, COL1A1, and SP7; as well as an increased expression of osteogenic cytochemical markers in cultures of ADSCs isolated from the falciform ligament, as compared to control.

Conclusion: It can thus be concluded, that FL-ADSCs are a relevant cell source for bone-related applications, given their high osteogenic capacity.

P024

Additive manufactured polyether-ether-ketone implants for orthopaedic applications and the promotion of integration of bone and soft tissue

Changning Sun[1], *Chaozong Liu*[2], *Dichen Li*[1]
[1]*Xi'an Jiaotong University, State Key Laboratory for Manufacturing System Engineering, Xi'an, China*
[2]*University College London, Division of Surgery & Interventional Science, London, United Kingdom*

Abstract Text

Polyether-ether-ketone (PEEK) is believed to be the next-generation biomedical material for orthopaedic implants that may replace metal materials because of its good biocompatibility, appropriate mechanical properties and radiolucency. Currently, PEEK implant represented by intervertebral fusion cage has been used successfully for many years. Till now, there is no customised PEEK orthopaedic implant made by additive manufacturing licensed for the market, although clinical trials have been increasingly reported. The poor integration between Poly-ether-ether-ketone (PEEK) with hard and soft tissue represents a major challenge of PEEK orthopaedic implant owing to its chemical inertness. Here we investigated the influence of hydroxyapatite (HA) contents and pore size of additive manufactured (AM) HA/PEEK composites scaffolds with HA content of 0, 20 wt% and 40 wt% on the integration with bone and soft tissues through cellular experiments and animal experiments. The cell experiment showed that the adhesion, proliferation, osteogenic differentiation and mineralization ability of mesenchymal stem cells (BMSCs) as well as the proliferation and adhesion of myofibroblasts on the PEEK/HA scaffolds were significantly improved. The in-vivo experiment demonstrated significant higher bone ingrowth and tighter adhesion of soft tissue in the HA/PEEK scaffolds. The ingrowth volume (24.3%) of 40 wt% HA/PEEK scaffold after implantation for 12 weeks was comparable to the bone ingrowth reported for metallic or ceramic scaffolds. The bonding strength between HA/PEEK scaffolds and soft tissue was dominated by the geometry dimension, while HA has a facilitative effect on the tight adhesion of the soft tissue to the PEEK-based composite scaffold, which is vital for avoiding postoperative effusion. The present study provides engineering-accessible design principles on material components and geometry of AM PEEK-based composites orthopaedic implant for improving the integration with bone and soft tissue. Typical clinical applications of PEEK-based 3D printed implant were carried out according to the design criteria.

P025

Bone Health in Men Receiving ADT for Prostate Cancer; A Pathway Optimisation

Victoria Osborn[1], *Emma Green*[1], *Margaret A Paggiosi*[1], *Derek Rosario*[2], *Eugene McCloskey*[1], *Michael Dixon*[2], *Janet E Brown*[1]
[1]*University of Sheffield, Oncology and Metabolism, Sheffield, United Kingdom*
[2]*Sheffield Teaching Hospitals NHS Foundation Trust, Urology, Sheffield, United Kingdom*

Abstract Text

Background

1 in 6 men will be diagnosed with Prostate Cancer (PC) during their lifetime, making it the most common cancer diagnosis in the UK [1]. Androgen Deprivation Therapy (ADT) is the standard of care treatment for prostate cancer; however it is associated with a deterioration in Bone Mineral Density (BMD), and consequently an increased risk of fracture [2,3]. Therefore, fracture risk assessment is crucial in these patients, and is monitored in standard practice using the Fracture Risk Assessment Tool (FRAX), and Dual Energy X-ray Absorptiometry (DXA) [3,4].

Brown et al produced updated guidance and recommendations for the management of PCa ADT induced bone loss [5]. Although published in updated NICE guidelines, implementation as part of standard of care has been interrupted due to the COVID-19 pandemic [6].

Purpose

This service evaluation aims to assess if completion of a musculoskeletal assessment using a standard questionnaire and DXA scan will aid the identification of men with prostate cancer undergoing ADT who are at higher risk of fracture. We will additionally assess whether the new recommended guidelines are carried out as standard of care within Sheffield teaching Hospitals (STH).

Methods

PC patients who have started ADT in the last 6 months will be given a questionnaire to complete which will give the evaluating team the information necessary to complete a FRAX assessment, as well as additional information relevant to the patient's bone health. Patients will also be asked to have a DXA scan to assess their bone mineral density. Staff at STH will be interviewed in order to determine their knowledge of the new guidelines and if they are routinely implemented.

Results

At the time of the conference, a submitted poster will provide early data results.

Conclusions

Conclusions will be made once data has been collected.

LB-P028

Investigating nanovibration as an intervention for the reversal of spinal cord injury-induced osteoporosis

Jonathan Williams[1,2,3], Paul Campsie[1], Richard Gibson[1], Carmen Huesa[4], James Windmill[5], Margaret Purcell[2], Matthew Dalby[6], Peter Childs[1], Sylvie Coupaud[2,7], John Riddell[2,3], Stuart Reid[1]
[1]University of Strathclyde, Centre for the Cellular Microenvironment - Department of Biomedical Engineering, Glasgow, United Kingdom
[2]Queen Elizabeth National Spinal Injuries Unit, Scottish Centre for Innovation in Spinal Cord Injury, Glasgow, United Kingdom
[3]University of Glasgow, School of Psychology and Neuroscience - College of Medical - Veterinary and Life Sciences, Glasgow, United Kingdom
[4]University of Glasgow, School of Infection and Immunity - College of Medical - Veterinary and Life Sciences, Glasgow, United Kingdom
[5]University of Strathclyde, Department of Electronic and Electrical Engineering, Glasgow, UK
[6]University of Glasgow, Centre for the Cellular Microenvironment, Glasgow, United Kingdom
[7]University of Strathclyde, Department of Biomedical Engineering, Glasgow, United Kingdom

Abstract Text

Introduction: Osteoporosis is a metabolic bone disease that disrupts the fine-tuned balance between bone resorption and formation, leading to reductions in both bone quantity and quality which lead to increased susceptibility to fracture. An extreme, time-accelerated form of this is observed in the paralysed limbs following complete spinal cord injury (SCI). *In vitro* nanoscale vibration (1kHz, 30-90nm amplitude) has been shown to drive differentiation of bone marrow-derived mesenchymal stem cells towards osteoblast-like phenotypes and enhance osteogenesis, while simultaneously inhibiting osteoclastogenesis.

Purpose: In this study, we investigated whether a controlled dose of nanovibration was effective in reversing established osteoporosis in rats with complete spinal cord transection.

Methods: A wearable device designed to deliver nanoscale vibration to the paralysed hindlimb long bones (proximal tibia) of rats, and record the transmitted vibration through the limb, was developed, optimised, and then characterised by laser interferometry.

The effect of nanovibration on the rat SCI osteoporosis model was investigated at 1 kHz and two amplitudes (40nm and 100nm). Nanovibration was applied for 4-hours/day, 5-days/week for 6 weeks. Trabecular and cortical bone microstructure were evaluated with micro-computed tomography. Serum bone formation and resorption markers were measured. Serum samples were subject to HILIC-mass spectrometry analysis and the results analysed using the KEGG database and Ingenuity Pathway Analysis software to identify metabolomic pathways.

Results and Conclusion: Laser interferometry confirmed the delivery of suitable nanovibration parameters to the long bones. This intervention did not reverse or attenuate SCI-induced osteoporosis. However, blood serum analysis indicated elevated concentration of bone formation marker P1NP in rats receiving 40nm amplitude nanovibration, suggesting increased synthesis of type 1 collagen. Other doses of nanovibrational stimulus may yet prove beneficial at attenuating/reversing osteoporosis, especially in less severe forms of osteoporosis.